

A General Framework For Modeling Gaussian Process with Qualitative and Quantitative Factors*

Linsui Deng and C. F. Jeff Wu[#]

School of Data Science, The Chinese University of Hong Kong, Shenzhen,
China

February 19, 2026

Abstract

Computer experiments involving both qualitative and quantitative (QQ) factors have attracted increasing attention. Gaussian process (GP) models have proven effective in this context by choosing specialized covariance functions for QQ factors. In this work, we extend the latent variable-based GP approach, which maps qualitative factors into a continuous latent space, by establishing a general framework to apply standard kernel functions to continuous latent variables. This approach provides a novel perspective for interpreting some existing GP models for QQ factors and introduces new covariance structures in some situations. The ordinal structure can be incorporated naturally and seamlessly in this framework. Furthermore, the Bayesian information criterion and leave-one-out cross-validation are employed for model selection and model averaging. The performance of the proposed method is comprehensively studied on several examples.

Keywords: Computer experiment; Ordinal variables; Uncertainty quantification; Latent variable; Bayesian information criterion; Leave-one-out cross validation

[#]Corresponding author. Email: jeffwu@cuhk.edu.cn

*This version is accepted for publication in *Technometrics*.

1 Introduction

Computer experiments have attracted increasing attention in science, engineering, and business due to their ability to model complex systems. However, the high computational cost of running these simulations often necessitates the use of surrogate models or emulators. Among these, Gaussian process (GP) modeling has emerged as a powerful approach because it can approximate the behavior of simulations accurately and efficiently (Santner et al., 2003). Recent developments have extended GP modeling to support a variety of input types, such as probability distributions (Bachoc et al., 2017) and functions (Li and Tan, 2022).

In many applications, the inputs of a computer experiment involve both quantitative and qualitative factors, commonly referred to as QQ inputs. For instance, in embankment system design, the inputs include one quantitative variable (shoulder distance from the centerline) and three qualitative variables (construction rate, Young's modulus of columns, and reinforcement stiffness) (Liu and Rowe, 2015; Deng et al., 2017). Similarly, modeling the thermal dynamics of a data center requires consideration of qualitative factors such as diffuser location, return air vent location, and rack heat load nonuniformity, along with quantitative factors like rack temperature rise, rack heat load, and total diffuser flow rate (Schmidt et al., 2005; Qian et al., 2008). These examples show the importance of developing GP models that work well with QQ inputs.

An essential step of GP modeling is the construction of the covariance function. In recent years, a number of covariance structures have been proposed and investigated to improve prediction accuracy for handling computer experiments with QQ inputs (Qian et al., 2008; Zhou et al., 2011; Deng et al., 2017; Zhang et al., 2020; Roustant et al., 2020; Garrido-Merchán and Hernández-Lobato, 2020; Tao et al., 2021; Xiao et al., 2021; Lin et al., 2024), as reviewed in Section 2.2. Nevertheless, there still lacks a general framework that ties these approaches together.

In this paper, we propose a general latent-variable-based framework for GP modeling with QQ inputs, built upon the latent variable approach proposed by [Zhang et al. \(2020\)](#). We show that this framework can include many existing covariance structures and allows a systematic development of new ones. This is achieved by applying different kernel functions to the latent variables, such as Gaussian, exponential, and linear kernels. We study identifiability conditions for the latent parameterization for these kernel settings. We further demonstrate how ordinal information can be integrated by imposing constraints on the latent variables. Given a variety of available kernel choices, we employ both leave-one-out cross-validation and the Bayesian information criterion (BIC) for model selection. Finally, we introduce a BIC-based model averaging strategy to robustly combine predictions from models employing different kernels.

The remainder of this paper is structured as follows. Section 2 introduces the general framework, establishes its connection to existing approaches, and provides the identifiability condition for the latent parameterization. Section 3 describes how to incorporate ordinal information within the framework. Estimation and prediction procedures are presented in Section 4. In Section 5, we describe the model selection and model averaging strategies. Section 6 provides comprehensive numerical comparisons. Section 7 summarizes the findings and makes further discussions.

2 Methodology

2.1 Framework

Consider a problem in which the response $Y(\mathbf{U}, \mathbf{V})$ has two types of inputs: $\mathbf{U} = (u_1, \dots, u_I)^\top$ are quantitative factors and $\mathbf{V} = (v_1, \dots, v_J)^\top$ are qualitative factors, with each v_j possessing a_j levels, i.e., $v_j \in \{1, 2, \dots, a_j\}$. We model the response using a GP, which is expressed

as

$$Y(\mathbf{U}, \mathbf{V}) = \mu + G(\mathbf{U}, \mathbf{V}),$$

where μ represents the constant mean term and $G(\mathbf{U}, \mathbf{V})$ is a zero-mean GP. The primary goal is to model the covariance between responses $Y(\mathbf{U}, \mathbf{V})$ and $Y(\mathbf{U}', \mathbf{V}')$ corresponding to two distinct inputs (\mathbf{U}, \mathbf{V}) and $(\mathbf{U}', \mathbf{V}')$. By utilizing the covariance kernel, we can make predictions for new inputs (Santner et al., 2003).

Existing approaches focus on choosing or proposing covariance structures that have some of the attributes: intuitive, interpretable, or computationally efficient (McMillan et al., 1999; Qian et al., 2008; Zhou et al., 2011; Deng et al., 2017). Motivated by the idea that qualitative variables can be represented by some underlying numerical values, Zhang et al. (2020) proposed that the j -th qualitative factor v_j corresponds to a latent vector $\mathbf{z}_{v_j}^{(j)} \in \mathbb{R}^{l_j}$, where $1 \leq l_j \leq a_j$. Following this formulation, we define the concatenated latent vector $\mathbf{Z}_V \in \mathbb{R}^{\sum_{j=1}^J l_j}$ as $\mathbf{Z}_V^\top = ((\mathbf{z}_{v_1}^{(1)})^\top, (\mathbf{z}_{v_2}^{(2)})^\top, \dots, (\mathbf{z}_{v_J}^{(J)})^\top)$. Using this framework, we can state that the response $Y(\mathbf{U}, \mathbf{V})$ for input (\mathbf{U}, \mathbf{V}) follows the same distribution as the response Y for input $(\mathbf{U}, \mathbf{Z}_V)$, i.e.,

$$Y(\mathbf{U}, \mathbf{V}) \stackrel{d}{=} Y(\mathbf{U}, \mathbf{Z}_V).$$

Given the GP assumption, this distributional equivalence holds if and only if their covariance functions are identical. Therefore, we propose to model the covariance function of $Y(\mathbf{U}, \mathbf{V})$, the original process of interest, using that of the continuous input $(\mathbf{U}, \mathbf{Z}_V)$ as follows

$$\begin{aligned} \text{Cov} \{Y(\mathbf{U}, \mathbf{V}), Y(\mathbf{U}', \mathbf{V}')\} &= \text{Cov} \{Y(\mathbf{U}, \mathbf{Z}_V), Y(\mathbf{U}', \mathbf{Z}'_V)\} \\ &= \sigma^2 \text{Corr} \{Y(\mathbf{U}, \mathbf{Z}_V), Y(\mathbf{U}', \mathbf{Z}'_V)\} \\ &= \sigma^2 K_{\mathbf{U}}(\mathbf{U}, \mathbf{U}') K_{\mathbf{Z}}(\mathbf{Z}_V, \mathbf{Z}'_V), \end{aligned} \tag{1}$$

where σ^2 denotes the variance, and $K_{\mathbf{U}}(\cdot, \cdot)$ and $K_{\mathbf{Z}}(\cdot, \cdot)$ are respectively kernel functions for

the quantitative factors and latent vectors associated with the qualitative factors. The last identity in (1) is based on the assumption that the effects of \mathbf{U} and \mathbf{V} on Y can be factorized. Both kernels satisfy the normalization condition $K_{\mathbf{U}}(\mathbf{U}, \mathbf{U}) = 1$ and $K_{\mathbf{Z}}(\mathbf{Z}, \mathbf{Z}) = 1$ for all $\mathbf{U} \in \mathbb{R}^I$ and $\mathbf{Z} \in \mathbb{R}^{\sum_{j=1}^J l_j}$. This framework is flexible because it can accommodate various kernel functions to capture diverse patterns.

While the assumption of latent vectors may initially appear restrictive, we show that this modeling framework integrates numerous established approaches (Qian et al., 2008; Deng et al., 2017; Zhang et al., 2020; Tao et al., 2021) as special cases. Furthermore, its inherent generality offers potential for further methodological advancements and applications.

2.2 Connection with existing approaches

In the following, we provide a detailed discussion to establish connections between the framework and some existing methods in the literature.

Multiplicative Linear Kernel. By imposing a multiplicative structure among qualitative variables and adopting the linear kernel for continuous variables (Rojo-Álvarez et al., 2018), the correlation defined by the latent vectors is

$$K_{\mathbf{Z}}(\mathbf{Z}_{\mathbf{V}}, \mathbf{Z}_{\mathbf{V}'}) = \prod_{j=1}^J K_j \left(\mathbf{z}_{v_j}^{(j)}, \mathbf{z}_{v'_j}^{(j)} \right) = \prod_{j=1}^J \left(\mathbf{z}_{v_j}^{(j)} \right)^\top \mathbf{z}_{v'_j}^{(j)}. \quad (2)$$

- Case I ($l_j = a_j$). The covariance structure proposed by Qian et al. (2008) is defined as

$$\text{Cov} \{Y(\mathbf{U}, \mathbf{V}), Y(\mathbf{U}', \mathbf{V}')\} = \sigma^2 \left\{ \prod_{j=1}^J \tau_{v_j, v'_j}^{(j)} \right\} K_{\mathbf{U}}(\mathbf{U}, \mathbf{U}'), \quad (3)$$

where $\left(\tau_{v, v'}^{(j)} \right)_{a_j \times a_j}$ are J semi-positive definite matrices with unit diagonal elements (SPDUDE). Here, $\tau_{v, v'}^{(j)}$ represents the correlation between levels v and v' for the j th

qualitative factor. By using the Cholesky decomposition (Pinheiro and Bates, 1996), we can represent $\tau_{v_j, v'_j}^{(j)}$ as the product of two column vectors, i.e.,

$$\tau_{v_j, v'_j}^{(j)} = \left(\mathbf{z}_{v_j}^{(j)} \right)^\top \mathbf{z}_{v'_j}^{(j)}. \quad (4)$$

In this way, the qualitative part in (3) can be equivalently expressed by (2). In addition, Zhou et al. (2011) suggested using hyperspherical parameterization to simplify the computations.

- Case II ($l_j < a_j$). Roustant et al. (2020) and Tao et al. (2021) explored the case where the length of the latent vector, l_j , is shorter than the number of levels, a_j , to impose a low-rank structure. This approach significantly reduces the number of hyperparameters and hence alleviates the estimation burden. Building on this, Tao et al. (2021) further introduced hyperspherical expressions to address computational challenges. However, the issue of identifiability was not thoroughly discussed (see Section 2.3).
- Case III (restricted correlation matrix). To simplify the complexity of the correlation matrix, one may assume specific structures, such as equal correlation considered in Qian et al. (2008). In our framework, this assumption can be transformed into restrictions on the latent variables. Specifically, it corresponds to a special case where independent noise is permitted, and one-dimensional latent vectors with equal elements are assigned.

Additive Linear Kernel. Deng et al. (2017) proposed to model covariance through imposing an additive structure for qualitative factors, which is then multiplied by the correlation attributed to quantitative factors. Our framework has a direct connection with theirs. Suppose $K_{\mathbf{Z}}(\cdot, \cdot)$ is the kernel function modified from a first-order additive GP process for continuous variables (Plate, 1999; Duvenaud et al., 2011), whose individual components employ a linear kernel. To establish this connection, we construct latent vectors satisfying (4).

The covariance in (1) becomes

$$\begin{aligned}
\sigma^2 \sum_{j=1}^J K_j \left(\mathbf{z}_{v_j}^{(j)}, \mathbf{z}_{v'_j}^{(j)} \right) K_{\mathbf{U}}(\mathbf{U}, \mathbf{U}') &= \sum_{j=1}^J \psi_j \sigma^2 \left\{ \left(\mathbf{z}_{v_j}^{(j)} \right)^\top \mathbf{z}_{v'_j}^{(j)} \right\} K_{\mathbf{U}}(\mathbf{U}, \mathbf{U}') \\
&= \sum_{j=1}^J \sigma_j^2 \tau_{v_j, v'_j}^{(j)} K_{\mathbf{U}}(\mathbf{U}, \mathbf{U}'),
\end{aligned} \tag{5}$$

where ψ_j denotes the weight satisfying $\sum_{j=1}^J \psi_j = 1$ and σ_j^2 represents the variance associated with the j th qualitative factor. The covariance in equation (5) is a special case of the covariance structure proposed by [Deng et al. \(2017\)](#), which has the form

$$\sum_{j=1}^J \sigma_j^2 \tau_{v_j, v'_j}^{(j)} K_{\mathbf{U}, j}(\mathbf{U}, \mathbf{U}'). \tag{6}$$

In their formulation, the kernel function $K_{\mathbf{U}, j}(\mathbf{U}, \mathbf{U}')$ varies across different quantitative factors j . In contrast, our approach uses a fixed kernel function for all quantitative factors.

Multiplicative Gaussian Kernel. [Zhang et al. \(2020\)](#) proposed and evaluated the kernel functions with a multiplicative structure and Gaussian kernel, which is defined as

$$K_{\mathbf{Z}}(\mathbf{Z}_{\mathbf{V}}, \mathbf{Z}_{\mathbf{V}'}) = \prod_{j=1}^J \exp \left\{ - \left\| \mathbf{z}_{v_j}^{(j)} - \mathbf{z}_{v'_j}^{(j)} \right\|^2 \right\}.$$

Although recognizing the potential to enhance its generality using other kernels, such as power exponential, Matérn, and lifted Brownian kernels, they did not go further to develop details for various choices of kernels. To apply other kernels, comprehensive investigations and empirical validations are essential to ensure their applicability in real-world applications. For instance, the linear kernel has distinct identifiability conditions and requires additional constraints compared to the Gaussian kernel, as will be presented in Section 2.3.

Pre-specified Latent Variable. A popular approach for modeling GP with QQ factors is

to encode qualitative variables into numerical vectors. For instance, [Garrido-Merchán and Hernández-Lobato \(2020\)](#) used one-hot encoding vectors of length a_j , where the v th element is $\mathbf{1}(v_j = v)$. In another instance, [Luo et al. \(2024\)](#) adopted similarity encoding ([Cerda et al., 2018](#)), which constructs feature vectors from pairwise similarities between qualitative variable levels. Once encoded, standard kernels for continuous variables can then be applied. Therefore, these two methods can be viewed as special cases of the general framework.

Non-separable Kernel. As shown in (6), [Deng et al. \(2017\)](#) suggested that the smoothness parameters of quantitative factors may vary across different qualitative factors. In addition, [Xiao et al. \(2021\)](#) assumed that these parameters vary across different levels within the same qualitative factor. [Lin et al. \(2024\)](#) partitioned the input space into several non-overlapping regions via a qualitative-factor-based tree and fitted a separate GP for each region. These methods could, in principle, be accommodated in our framework by relaxing the factorization assumption in (1) and capturing interactions between QQ factors using non-separable kernels, such as higher-order additive GP ([Duvenaud et al., 2011](#)) or tree GP ([Gramacy and Lee, 2008](#)). While such extensions are feasible, the need for careful kernel specification and the substantially greater modeling complexity would likely limit their practical benefits.

To summarize, the relevant methodologies fall into three categories: (i) data-driven latent variables, summarized in Table 1; (ii) prespecified latent variables, such as one-hot and similarity encoding; and (iii) approaches that model interactions between QQ factors. The first two categories can be readily interpreted within the proposed framework, whereas the third cannot be fully explained due to the presence of interactions.

Finally, another line of research adopts a matrix-first perspective by structurally parameterizing the correlation matrix of the qualitative factors $\left(\tau_{v,v'}^{(j)}\right)$, which directly extends [Qian et al. \(2008\)](#). [Roustant et al. \(2020\)](#) employed block-structured correlation matrices to impose group-level structure on the correlations among levels of each qualitative input. [Saves](#)

Type	Kernel Functions				
	linear	equal	Gaussian	exponential	linear
	full-dim	correlation	low-dim	low-dim	low-dim
multiplicative	▲○●	▲●	■□●	■●	□●
additive	△●	△●	●	●	●

Table 1: Comparison of methods explicitly incorporating specific kernel functions and structures. We consider both multiplicative and additive relationships between qualitative variables. Different colors represent different methods: ● indicates our framework; ▲ corresponds to the method proposed by [Qian et al. \(2008\)](#); ○ refers to the method by [Zhou et al. \(2011\)](#); △ represents the approach by [Deng et al. \(2017\)](#); ■ and □ denote latent variable-based approaches studied in [Zhang et al. \(2020\)](#) and [Tao et al. \(2021\)](#), respectively.

[et al. \(2023\)](#) constructed correlation matrices through generalized continuous exponential kernels, which have a generalized form and include the continuous relaxation and Gower distance approaches as special cases. Our approach adopts a different perspective by using latent representations for the qualitative factors and induces correlations implicitly through standard kernels defined on the latent space.

2.3 Identifiability

Since the relationship between any inputs can be fully characterized by (1), it is crucial to examine the conditions on latent vectors and kernel functions that guarantee uniqueness. To address this, we formalize the concept of parameterization equivalence.

Definition 1 (Parameterization Equivalence). *We say the latent parameterization $\{\mathbf{Z}_V\}$ under the kernel $K_Z(\cdot, \cdot)$ and the latent parameterization $\{\mathbf{W}_V\}$ under the kernel $K_W(\cdot, \cdot)$ are equivalent if $K_Z(\mathbf{Z}_V, \mathbf{Z}_{V'}) = K_W(\mathbf{W}_V, \mathbf{W}_{V'})$ for all $V, V' \in \times_{j=1}^J \{1, 2, \dots, a_j\}$.*

To ensure the covariance in (1) is well defined, $K_Z(\cdot, \cdot)$ is required to be a Mercer kernel ([Mercer, 1909](#); [Bach and Jordan, 2002](#)). Specifically, $K_Z(\cdot, \cdot)$ is a function from $\mathbb{R}^{\sum_{j=1}^J l_j} \times \mathbb{R}^{\sum_{j=1}^J l_j}$ to \mathbb{R} , and for any n inputs $\mathbf{Z}_1, \dots, \mathbf{Z}_n$, the matrix $(K_Z(\mathbf{Z}_i, \mathbf{Z}_j))_{n \times n}$ must be positive

semidefinite. Common examples of Mercer kernels include the Gaussian, exponential, and Matérn kernels. Furthermore, when the kernel exhibits certain separability properties, the linear kernel is very flexible and capable of representing a wide range of kernels.

Theorem 1. *Suppose the structure between different qualitative variables is either multiplicative*

$$K_{\mathbf{Z}}(\mathbf{Z}_V, \mathbf{Z}_{V'}) = \prod_{j=1}^J K_j^{\mathbf{Z}} \left(\mathbf{z}_{v_j}^{(j)}, \mathbf{z}_{v'_j}^{(j)} \right) \quad (7)$$

or additive

$$K_{\mathbf{Z}}(\mathbf{Z}_V, \mathbf{Z}_{V'}) = \sum_{j=1}^J \psi_j K_j^{\mathbf{Z}} \left(\mathbf{z}_{v_j}^{(j)}, \mathbf{z}_{v'_j}^{(j)} \right) \quad (8)$$

with $\sum_{j=1}^J \psi_j = 1$. There always exists a latent parameterization $\{\mathbf{W}_V\}$ with $\mathbf{w}_{v_j}^{(j)} \in \mathbb{R}^{a_j}$ under the kernel $K_{\mathbf{W}}(\cdot, \cdot)$ with $K_j^{\mathbf{W}}(\cdot, \cdot)$ being the linear kernel, that is equivalent to the latent parameterization $\{\mathbf{Z}_V\}$ with $\mathbf{z}_{v_j}^{(j)} \in \mathbb{R}^{l_j}$ under the kernel $K_{\mathbf{Z}}(\cdot, \cdot)$ with $K_j^{\mathbf{Z}}(\cdot, \cdot)$ being any Mercer kernel.

Remark 1. *When the kernel is non-separable, all qualitative variables are integrated into a single variable with $\prod_{j=1}^J a_j$ levels, where each level corresponds to a unique combination of the original qualitative variables. In this way, non-separable kernels can be represented by some latent parameterization under linear kernels by applying Theorem 1.*

Theorem 1 and Remark 1 hold because we use a linear kernel for the latent representation $\{\mathbf{W}_V\}$. The proof of Theorem 1 is provided in the Appendix. The reverse of Theorem 1 does not hold. For instance, some latent parameterizations under the linear kernel cannot be represented by the Gaussian kernel because the linear kernel can accommodate negative correlations, whereas the Gaussian kernel is restricted to modeling positive correlations only. In other words, when $l_j = a_j$, the linear kernel exhibits greater flexibility compared to other kernels. Remark 1 addresses the case where kernels among qualitative variables are

non-separable. A similar approach was proposed in [Oune and Bostanabad \(2021\)](#) using the Gaussian kernel. However, the increased number of levels results in more parameters, which makes parameter estimation more difficult.

Although such a reparameterization always exists, if the true underlying kernel structure follows or approximately follows a Gaussian kernel with $l_j < a_j$, it may be possible to recover the structure using fewer parameters, which can reduce redundancy and variability while improving computational efficiency.

With a fixed kernel function $K_{\mathbf{Z}}(\cdot, \cdot)$, different latent vectors can produce identical covariance structures. Hence, examining the uniqueness of latent vectors and identifying the essential components that define the covariance is important. This identifiability issue is dependent on the specific kernel function employed.

To begin with, understanding the parameterization problem from a geometric perspective provides valuable insights. For the linear kernel, equivalence under orthogonal transformations corresponds to isometries in the inner product space, where angles and distances are preserved. Rotations about the origin and reflections across any plane passing through the origin maintain the relationships between vectors. For Gaussian kernels (later extended to isotropic kernels), equivalence corresponds to isometries in the distance space, where distances remain invariant. In addition to rotation and reflection, translations also preserve the relative distances between vectors.

Below, we provide an identifiability condition for the linear and isotropic kernels when $I = 0$ and $J = 1$, where I is the total number of quantitative factors and J is the total number of qualitative factors. An isotropic kernel is a kernel function $K(\mathbf{x}, \mathbf{x}')$ that depends only on the relative Euclidean distance between two inputs, i.e., $K(\mathbf{x}, \mathbf{x}') = \mathcal{K}(d)$, where $d = \|\mathbf{x} - \mathbf{x}'\|_2$ and kernel generating function $\mathcal{K}(\cdot)$ is a nonnegative and monotonically decreasing. Here, we take $I = 0$ (i.e., there is no quantitative factor) because the identifiability issue arises only

from the latent representations associated with qualitative factors. For the case $J > 1$, under the multiplicative structure in (7) or the additive structure in (8) considered in Theorem 1, identifiability can be established by examining each qualitative factor individually.

Proposition 1 (Identifiability for linear kernel). *Consider the latent parameterization $\{\mathbf{Z}_v\}$ such that $(\mathbf{z}_1^{(1)}, \dots, \mathbf{z}_{l_1}^{(1)})$ is full rank and $\|\mathbf{z}_v\|_2 = 1$ for all $1 \leq v \leq a_1$.*

- (a) *There always exists a unique parameterization $\{\mathbf{W}_v\}$ satisfying $w_{v,l}^{(j)} = 0$ for all $l > v$ and $w_{v,v}^{(j)} > 0$ for $1 \leq v \leq l_1$ that is equivalent to $\{\mathbf{Z}_v\}$ under the linear kernel.*
- (b) *$\{\mathbf{W}_v\}$ can be deployed to hyperspherical coordinates through*

$$w_{v,l}^{(1)} = \cos(\theta_{v,l}^{(1)}) \prod_{\iota=1}^{l-1} \sin(\theta_{v,\iota}^{(1)}) \text{ for } 1 \leq l < l_1 - 1 \text{ and } w_{v,l}^{(1)} = \prod_{\iota=1}^l \sin(\theta_{v,\iota}^{(1)}) \text{ for } l = l_1 - 1,$$

with the constraint $0 \leq \theta_{v,l}^{(1)} \leq \pi$ for $1 \leq l < \min(v, l_1)$, $0 \leq \theta_{v,l_1-1}^{(1)} \leq 2\pi$ for $v \geq l_1$ and $\theta_{v,l}^{(1)} = 0$ for $v \leq l$, where $v \in \{1, \dots, a_1\}$.

Proposition 2 (Identifiability for isotropic kernel). *Consider the latent parameterization $\{\mathbf{Z}_v\}$ such that $(\mathbf{z}_2^{(1)} - \mathbf{z}_1^{(1)}, \dots, \mathbf{z}_{l_1+1}^{(1)} - \mathbf{z}_1^{(1)})$ is full rank. There always exists a unique parameterization $\{\mathbf{W}_v\}$ satisfying $w_{v,l}^{(1)} = 0$ for all $l \geq v$ and $w_{v,v-1}^{(1)} > 0$ for $2 \leq v \leq l_1 + 1$ that is equivalent to $\{\mathbf{Z}_v\}$ under the isotropic kernel.*

The proofs of Propositions 1 and 2 are provided in the Appendix. For the linear kernel, the hyperspherical coordinate transformation simplifies the optimization process subject to the norm constraint for the latent vectors (see Lemma S1). Compared to Zhou et al. (2011), we allow $l_j \leq a_j$ whereas they restrict $l_j = a_j$. Consequently, additional attention is paid to determine the range of the angles. Specifically, their range of angles is $[0, \pi]$, whereas we require the additional condition $0 \leq \theta_{v,l_1-1}^{(1)} \leq 2\pi$ for $v \geq l_1$. Note that Zhang et al. (2020) and Yerramilli et al. (2023) claimed that the Gaussian kernel is invariant under translation and rotation. However, as stated in Proposition 2, to ensure uniqueness also requires translation

invariance. For instance, when $l_j = 2$ and $a_j > 3$, we require $w_{3,2}^{(1)} > 0$. Finally, our approach can extend the scope to encompass any isotropic kernel.

3 Ordinal variable

For ordinal variables, adjacent levels are generally expected to exhibit closer relationships. [Luo et al. \(2024\)](#) treats ordinal variables as nominal when the number of levels is small, and as continuous variables constrained to integer values when large. This empirical rule is straightforward to apply but may either overlook the underlying ordinal structure or be applicable only when the ordinal variable takes integer values. [Qian et al. \(2008\)](#) proposed two approaches for modeling ordinal correlations: one applies constraints to the correlation matrix, while the other transforms the ordinal scale into a continuous variable and defines correlations based on the transformed values. Although the two approaches provide valuable conceptual schemes, they do not offer specific algorithms for practical implementation. [Roustant et al. \(2020\)](#) developed upon the second approach of [Qian et al. \(2008\)](#) by applying a cosine kernel to the distances between transformed values. However, their method handles nominal and ordinal variables separately and regards them as two distinct types.

Our framework is directly applicable to ordinal variables by imposing order constraints on latent variables. Specifically, for the isotropic kernel, we consider a one-dimensional latent vector $\mathbf{z}^{(j)}$ (or scalar latent variable; we use the same notation for simplicity) and require that $0 = z_{1,1}^{(j)} \leq z_{2,1}^{(j)} \leq \dots \leq z_{a_j,1}^{(j)}$. This constraint ensures that the relative distances between the latent variables preserve the ordinal information. As discussed in Section 2.3, under the linear kernel, the correlation between two latent vectors is determined by the angle between them. This observation motivates our use of angles in hyperspherical coordinates to encode ordinal information. Specifically, we define $z_{v,1}^{(j)} = \cos(\theta_{v,1}^{(j)})$ and $z_{v,2}^{(j)} = \sin(\theta_{v,2}^{(j)})$ with the

constraint $0 = \theta_{1,1}^{(j)} \leq \theta_{2,1}^{(j)} \leq \dots \leq \theta_{a_j,1}^{(j)} \leq \pi$, where $\theta_{v,1}^{(j)}$ denotes the angles associated with the v th levels of the j th qualitative variable. This transformation effectively captures one-dimensional ordinal structure within a two-dimensional latent space.

To simplify optimization under ordinal constraints, we reparameterize the ordinal structure using non-negative increments. Specifically, for the isotropic kernel, we define $z_{v,1}^{(j)} = \sum_{\iota=1}^v \Delta_{\iota}^{(\mathbf{z},j)}$, where $\Delta_1^{(\mathbf{z},j)} = 0$ and $\Delta_{\iota}^{(\mathbf{z},j)} \geq 0$, $2 \leq \iota \leq a_j$. In this case, the ordinal constraint is transformed into a box-constrained optimization problem (Carpenter et al., 2017), which can be efficiently solved by the L-BFGS-B algorithm (Byrd et al., 1995). For notation consistency, we represent $\theta_{v,1}^{(j)} = \sum_{\iota=1}^v \Delta_{\iota}^{(\boldsymbol{\theta},j)}$ for the linear kernel, where $\Delta_1^{(\boldsymbol{\theta},j)} = 0$, $\Delta_{\iota}^{(\boldsymbol{\theta},j)} \geq 0$, $2 \leq \iota \leq a_j$, and $\theta_{a_j,1}^{(j)} = \sum_{\iota=1}^{a_j} \Delta_{\iota}^{(\boldsymbol{\theta},j)} < \pi$. The parameters are optimized using an adaptive barrier algorithm (Lange, 1999, Chapter 16.3). A summary of the reparameterizations, along with the identifiability conditions and the number of parameters, is shown in Table 2.

As shown in Table 2, the latent representations $\{\mathbf{Z}_V\}$ are uniquely determined by these reparameterized parameters, provided under the identifiability conditions. For convenience, we collectively denote these reparameterized parameters as $\{\Omega_V\}$, with specific forms based on the kernel and variable type: for a linear kernel, $\{\Omega_V\} = \{\theta_{v,\iota}^{(j)}\}$ (nominal) or $\{\Omega_V\} = \{\Delta_{\iota}^{(\boldsymbol{\theta},j)}\}$ (ordinal); for an isotropic kernel, $\{\Omega_V\} = \{\mathbf{Z}_V\}$ (nominal) or $\{\Omega_V\} = \{\Delta_{\iota}^{(\mathbf{z},j)}\}$ (ordinal). Imposing the identifiability conditions is achieved by restricting $\{\Omega_V\}$ to a specific region \mathcal{M}_{Ω} .

It is helpful to illustrate how different kernel choices for qualitative variables impose fundamentally different low-dimensional structures. Consider a simple scenario with a single ordinal qualitative variable having $a_1 = 3$ levels and latent dimension $l_1 = 1$. Let $\tau_{v,v'}^{(1)} = K_{\mathbf{Z}} \left(\mathbf{z}_v^{(1)}, \mathbf{z}_{v'}^{(1)} \right)$ denote the kernel-induced correlation between levels v and v' of the qualitative variable. We reparameterize the latent embeddings via non-negative increments as $\theta_{1,1}^{(1)} = \Delta_1^{(\boldsymbol{\theta},1)} = 0$, $\theta_{2,1}^{(1)} = \Delta_2^{(\boldsymbol{\theta},1)}$, $\theta_{3,1}^{(1)} = \Delta_2^{(\boldsymbol{\theta},1)} + \Delta_3^{(\boldsymbol{\theta},1)}$, and similarly $z_{1,1}^{(1)} = \Delta_1^{(\mathbf{z},1)} = 0$, $z_{2,1}^{(1)} = \Delta_2^{(\mathbf{z},1)}$,

Kernel Type	Variable Type	$K_j(\mathbf{z}_v^{(j)}, \mathbf{z}_{v'}^{(j)})$	Reparameterization of $z_{v,l}^{(j)}$	Identifiability Condition \mathcal{M}_Ω	Num. of Para. $\mathcal{P}_j(l_j; a_j)$
Nominal		$\left(\mathbf{z}_v^{(j)}\right)^\top \mathbf{z}_{v'}^{(j)}$	$\cos\left(\theta_{v,l}^{(j)}\right) \prod_{\ell=1}^{l-1} \sin\left(\theta_{v,\ell}^{(j)}\right)$ for $1 \leq l < l_j - 1$	$0 \leq \theta_{v,l}^{(j)} \leq \pi$ for $1 \leq l < \min(v, l_j)$	$(a_j - 1)(l_j - 1)$
			$\prod_{\ell=1}^l \sin\left(\theta_{v,\ell}^{(j)}\right)$ for $l = l_j - 1$	$0 \leq \theta_{v,l_j-1}^{(j)} \leq 2\pi$ for $v \geq l_j$ $\theta_{v,l}^{(j)} = 0$ for $v \leq l$	
Linear		$\left(\mathbf{z}_v^{(j)}\right)^\top \mathbf{z}_{v'}^{(j)}$	$\cos\left(\sum_{\ell=1}^v \Delta_\ell^{(\theta,j)}\right)$ for $l = 1$	$\Delta_1^{(\theta,j)} = 0$	$a_j - 1$
			$\sin\left(\sum_{\ell=1}^v \Delta_\ell^{(\theta,j)}\right)$ for $l = 2$	$\Delta_v^{(\theta,j)} \geq 0$ $0 \leq \sum_{\ell=1}^{a_j} \Delta_\ell^{(\theta,j)} \leq \pi$	
Isotropic	Nominal	$\mathcal{K}_j\left(\left\ \mathbf{z}_v^{(j)} - \mathbf{z}_{v'}^{(j)}\right\ _2\right)$	$z_{v,l}^{(j)}$	$z_{v,v-1}^{(j)} > 0$ $z_{v,l}^{(j)} = 0$ for $l \geq v$	$(2a_j - l_j - 1)l_j/2$
	Ordinal ($l_j = 1$)	$\mathcal{K}_j\left(\left\ \mathbf{z}_v^{(j)} - \mathbf{z}_{v'}^{(j)}\right\ _2\right)$	$\sum_{\ell=1}^v \Delta_\ell^{(\mathbf{z},j)}$ for $l = 1$	$\Delta_1^{(\mathbf{z},j)} = 0$ $\Delta_v^{(\mathbf{z},j)} \geq 0$	$a_j - 1$

Table 2: Summary of reparameterizations $\{\Omega_{\mathbf{V}}\}$ and ranges \mathcal{M}_Ω for different qualitative variable types under different kernel structures.

$z_{3,1}^{(1)} = \Delta_2^{(\mathbf{z},1)} + \Delta_3^{(\mathbf{z},1)}$. Under the linear kernel, the correlations satisfy $\tau_{1,3}^{(1)} = \tau_{1,2}^{(1)}\tau_{2,3}^{(1)} - \{1 - (\tau_{1,2}^{(1)})^2\}^{1/2}\{1 - (\tau_{2,3}^{(1)})^2\}^{1/2}$, which arises from the cosine law on the unit circle in two-dimensional space. In contrast, for the Gaussian kernel, the correlation must satisfy $\tau_{1,3}^{(1)} = \tau_{1,2}^{(1)}\tau_{2,3}^{(1)} \exp\{-2(\log \tau_{1,2}^{(1)})^{1/2}(\log \tau_{2,3}^{(1)})^{1/2}\}$, which follows from solving $\Delta_2^{(\mathbf{z},1)}$ and $\Delta_3^{(\mathbf{z},1)}$ given $\tau_{1,2}^{(1)}$ and $\tau_{2,3}^{(1)}$, and then substituting them into the expression for $\tau_{1,3}^{(1)}$. These expressions reveal that even if the pairwise similarities between adjacent levels are identical, the implied similarity between non-adjacent levels can differ substantially depending on the kernel choice. As a result, while [Roustant et al. \(2020\)](#) recommended the linear kernel to capture potential negative correlation and ordinal information simultaneously, this choice may be suboptimal if Gaussian or other kernels are more suitable for capturing the underlying structure. In Section 5, we will explore model selection and model averaging techniques to determine the appropriate kernel for analysis and to combine predictions for enhanced performance.

4 Estimation and prediction

As shown in (1), the kernels for the quantitative and qualitative factors are user-specified.

By following standard practice, we employ the Gaussian kernel for the quantitative factors.

Denote the unknown parameters within the kernel function as Φ . We have

$$K_{\mathbf{U}}(\mathbf{U}, \mathbf{U}') = K_{\mathbf{U}}(\mathbf{U}, \mathbf{U}' \mid \Phi) = \exp \left\{ - \sum_{i=1}^I \phi_i (u_i - u'_i)^2 \right\},$$

where $\Phi = (\phi_1, \phi_2, \dots, \phi_I)$. Other popular kernels, such as the exponential kernel and the Matérn kernel, can also be used.

In the following, we focus on the category of data-driven latent variables described in Section 2.2 because the estimated latent variables provide valuable insights into the similarities between different levels. Some of the suggested kernels for qualitative variables are listed in Table 1. We examine combinations of the multiplicative or additive structure, as defined in (7) and (8), with different choices of $K_j^{\mathbf{Z}}(\cdot, \cdot)$, including Gaussian, exponential, and linear kernels. We consider one and two dimensions for the Gaussian and exponential kernels, and two and three dimensions for the linear kernel. When ordinal information is present, we can also incorporate the corresponding method for comparison.

Estimation. Suppose there are n response values $\mathbf{Y} = (Y_1, \dots, Y_n)^\top$ corresponding to input values $\mathbf{D} = \{(\mathbf{U}_1, \mathbf{V}_1), (\mathbf{U}_2, \mathbf{V}_2), \dots, (\mathbf{U}_n, \mathbf{V}_n)\}$. The log-likelihood function up to an additive constant is

$$l(\mu, \sigma^2, \Phi, \{\Omega_{\mathbf{V}}\}) = -\frac{1}{2} \left\{ n \log(\sigma^2) + \log |\mathbf{R}| + (\mathbf{Y} - \mu \mathbf{1})^\top \mathbf{R}^{-1} (\mathbf{Y} - \mu \mathbf{1}) / \sigma^2 \right\}, \quad (9)$$

where $\mathbf{1}$ is a vector of length n with elements one, $|\cdot|$ is the determinant, and $\{\Omega_{\mathbf{V}}\}$ are reparameterized parameters. The latent parameterization $\{\mathbf{Z}_{\mathbf{V}}\}$ is calculated using the in-

formation in column 4 of Table 2. Then, \mathbf{R} is the correlation matrix whose (i, j) th element is calculated through $K_{\mathbf{U}}(\mathbf{U}_i, \mathbf{U}_j | \Phi)K_{\mathbf{Z}}(\mathbf{Z}_{\mathbf{V}_i}, \mathbf{Z}_{\mathbf{V}_j})$. In our experiments, the computation of \mathbf{R}^{-1} is sometimes numerically unstable due to ill-conditioning. Following Peng and Wu (2014), we use a nugget term in kriging to improve its conditioning, which adds a small positive constant to the diagonal of \mathbf{R} and ensure that the smallest eigenvalue is above a prescribed threshold ϵ . Specifically, we consider a sequence of candidate thresholds, e.g., $\epsilon \in \{10^{-1}, 10^{-2}, \dots, 10^{-8}\}$, select the value that minimizes the negative log-likelihood, and then replace \mathbf{R} by $\mathbf{R} + \delta \mathbf{I}_n$, where $\delta = \max\{0, \epsilon - \lambda_{\min}(\mathbf{R})\}$, with $\lambda_{\min}(\mathbf{R})$ denoting the smallest eigenvalue of the original correlation matrix, and $\mathbf{I}_n \in \mathbb{R}^{n \times n}$ being the identity matrix. Given Φ and $\{\mathbf{Z}_{\mathbf{V}}\}$, $\hat{\mu}$ and $\hat{\sigma}^2$ are estimated by

$$\hat{\mu} = (\mathbf{1}^\top \mathbf{R}^{-1} \mathbf{1})^{-1} \mathbf{1}^\top \mathbf{R}^{-1} \mathbf{Y} \quad \text{and} \quad \hat{\sigma}^2 = (\mathbf{Y} - \hat{\mu} \mathbf{1})^\top \mathbf{R}^{-1} (\mathbf{Y} - \hat{\mu} \mathbf{1}) / n.$$

Plug the estimated mean and variance into the log-likelihood function, and then the remaining parameters are estimated through

$$\left(\hat{\Phi}, \{\hat{\Omega}_{\mathbf{V}}\} \right) = \arg \min_{\Phi, \{\Omega_{\mathbf{V}} \in \mathcal{M}_{\Omega}\}} \{n \log(\hat{\sigma}^2) + \log |\mathbf{R}|\},$$

where \mathcal{M}_{Ω} denotes the region describing identifiability conditions, as provided in Table 2.

Prediction. We can perform prediction and interpolation in the same manner as in ordinary kriging for quantitative-only variables. Denote the estimated parameters as $\hat{\mu}$, $\hat{\sigma}^2$, $\hat{\Phi}$, and $\{\hat{\Omega}_{\mathbf{V}}\}$. Then, estimated latent representations $\{\hat{\mathbf{Z}}_{\mathbf{V}}\}$ are obtained via using the information in column 4 of Table 2. The estimated correlation matrix, $\hat{\mathbf{R}}$, has its (i, j) th entry $K_{\mathbf{U}}(\mathbf{U}_i, \mathbf{U}_j | \hat{\Phi})K_{\mathbf{Z}}(\hat{\mathbf{Z}}_{\mathbf{V}_i}, \hat{\mathbf{Z}}_{\mathbf{V}_j})$. For a new input $(\mathbf{U}^*, \mathbf{V}^*)$, we predict its response and

corresponding variance as follows:

$$\widehat{Y}(\mathbf{U}^*, \mathbf{V}^*) = \widehat{\mu} + \widehat{\mathbf{r}}^\top \widehat{\mathbf{R}}^{-1}(\mathbf{Y} - \widehat{\mu}\mathbf{1}) \text{ and } s^2(\mathbf{U}^*, \mathbf{V}^*) = \widehat{\sigma}^2 \left\{ 1 - \widehat{\mathbf{r}}^\top \widehat{\mathbf{R}}^{-1} \widehat{\mathbf{r}} + \frac{(\widehat{\mathbf{r}}^\top \widehat{\mathbf{R}}^{-1} \mathbf{1} - 1)^2}{\mathbf{1}^\top \widehat{\mathbf{R}}^{-1} \mathbf{1}} \right\},$$

where $\widehat{\mathbf{r}} = (r_1, \dots, r_n)$ with $r_i = K_{\mathbf{U}}(\mathbf{U}_i, \mathbf{U}^* | \widehat{\Phi}) K_{\mathbf{Z}}(\widehat{\mathbf{Z}}_{\mathbf{V}_i}, \widehat{\mathbf{Z}}_{\mathbf{V}^*})$.

5 Model selection and model averaging

The general framework can induce different models by selecting different kernels and varying the dimension of latent spaces (see Table 1). Suppose there are K candidate models, denoted by $\{\mathcal{M}_1, \dots, \mathcal{M}_K\}$. A natural question then arises: How should we determine which kernel to use?

Motivated by the model selection problem in GP with quantitative inputs, we propose two types of criteria to address this question. The first type utilizes leave-one-out cross-validation (LOOCV), which has been commonly used for kernel selection in Gaussian processes with quantitative inputs (Dubrule, 1983; Rasmussen and Williams, 2006) and for simulator selection (Hung et al., 2023). The second type employs the Bayesian information criterion, BIC (Schwarz, 1978), which has been shown to provide satisfactory selection performance in a different context (Chen et al., 2024).

5.1 LOOCV-based model selection

The LOOCV procedure proceeds as follows. The leave-one-out prediction involves fitting the model while leaving one observation out, then calculating the error based on the model's performance when making predictions using the fitted model. We calculate the LOOCV score for input i of each model \mathcal{M}_k in the prediction step, rather than in the estimation

step. Specifically, we calculate the LOOCV score of \mathcal{M}_k as follows:

$$\widehat{S}_{\mathcal{M}_k} = \frac{1}{n} \sum_{i=1}^n \widehat{S}_{\mathcal{M}_k,(i)}, \quad \text{with} \quad \widehat{S}_{\mathcal{M}_k,(i)} = L \left(Y_i; \widehat{\mu}_{\mathcal{M}_k,(i)}, \widehat{\sigma}_{\mathcal{M}_k,(i)}^2 \right),$$

where $\widehat{\mu}_{\mathcal{M}_k,(i)}$ and $\widehat{\sigma}_{\mathcal{M}_k,(i)}^2$ are estimated mean and variance using $\mathbf{D} \setminus \{(\mathbf{U}_i, \mathbf{V}_i)\}$. The function $L(y; \mu, \sigma^2)$ denotes a user-defined marginal error measure for an observation y under the assumption that y follows a normal distribution with mean μ and variance σ^2 . According to [Rasmussen and Williams \(2006\)](#), the leave-one-out estimated mean and variance have closed-form solutions, given by

$$\widehat{\mu}_{\mathcal{M}_k,(i)} = Y_i - \left(\widehat{\mathbf{R}}^{-1} \mathbf{Y} \right)_i / \left(\widehat{\mathbf{R}}^{-1} \right)_{ii} \quad \text{and} \quad \widehat{\sigma}_{\mathcal{M}_k,(i)}^2 = 1 / \left(\widehat{\mathbf{R}}^{-1} \right)_{ii},$$

where $(\cdot)_i$ is the i th element of vector and $(\cdot)_{ij}$ is the (i, j) th element of matrix, respectively.

We then choose the model minimizing the LOOCV score. In practice, we have two methods using different error measurements $L(y; \mu, \sigma^2)$:

1. The $\text{LOOCV}_{\text{log-lik}}$ uses the negative log-likelihood of the normal distribution, defined as $L(y; \mu, \sigma^2) = \{\log(2\pi\sigma^2)\}/2 + (y - \mu)^2/2\sigma^2$.
2. The LOOCV_{l_2} measures the l_2 loss between the predicted value $\widehat{\mu}_{\mathcal{M}_k,(i)}$ and the observed value Y_i , defined as $L(y; \mu, \sigma^2) = (y - \mu)^2$.

5.2 BIC-based model selection

The BIC_{MSel} method selects the model that minimizes the BIC criterion as the final model.

When the multiplicative structure is assigned between different qualitative variables, the

BIC is defined as

$$\widehat{\text{BIC}}_{\mathcal{M}_k} = -2l\left(\widehat{\mu}, \widehat{\sigma}^2, \widehat{\Phi}, \{\widehat{\Omega}_{\mathbf{V}}\}\right) + \left(2 + I + \sum_{j=1}^J \mathcal{P}_j(l_j; a_j)\right) \ln(n), \quad (10)$$

where $\widehat{\mu}, \widehat{\sigma}^2, \widehat{\Phi}$ and $\{\widehat{\Omega}_{\mathbf{V}}\}$, $2 + I + \sum_{j=1}^J \mathcal{P}_j(l_j; a_j)$ are the number of parameters, including two parameters for mean and variance, I parameters for the scale parameter for the quantitative variables and $\sum_{j=1}^J \mathcal{P}_j(l_j; a_j)$ parameters defined in Table 2, for the qualitative variables. The first term in (10) evaluates the goodness-of-fit of the model, while the second term imposes a penalty for model complexity.

When an additive structure is employed, the number of parameters increases by $J - 1$, as the relative weights $\{\psi_j\}$, shown in (8), are also considered unknown parameters and are subject to the constraint $\sum_{j=1}^J \psi_j = 1$.

5.3 BIC-based model average

Treating $\{\mathcal{M}_k\}$ as prior models with equal probabilities, we can leverage the results given by different models and hence make predictions more robustly. Following [Claeskens and Hjort \(2008\)](#), we can obtain the posterior probability of each model \mathcal{M}_k as follows:

$$p(\mathcal{M}_k \mid \mathbf{D}) \propto p(\mathbf{D} \mid \mathcal{M}_k)p(\mathcal{M}_k) \approx \exp\left(-\widehat{\text{BIC}}_{\mathcal{M}_k}/2\right) p(\mathcal{M}_k).$$

Therefore, the final model of BIC_{MAvr} is a weighted average of different models, where the weights are determined by their BIC values. To derive the prediction and associated uncertainty from the final model, let $\widehat{Y}_{\mathcal{M}_k}$ denote the value predicted by model \mathcal{M}_k , and let $s_{\mathcal{M}_k}^2$ be the corresponding predictive variance for a new input $(\mathbf{U}^*, \mathbf{V}^*)$. The final predicted value

and variance are then given by

$$\widehat{Y}(\mathbf{U}^*, \mathbf{V}^*) = \sum_{k=1}^K w_{\mathcal{M}_k} \widehat{Y}_{\mathcal{M}_k}, \quad \text{and} \quad s^2(\mathbf{U}^*, \mathbf{V}^*) = \sum_{k=1}^K w_{\mathcal{M}_k} \sqrt{s_{\mathcal{M}_k}^2 + \left\{ \widehat{Y}(\mathbf{U}^*, \mathbf{V}^*) - \widehat{Y}_{\mathcal{M}_k} \right\}^2}.$$

where $w_{\mathcal{M}_k} \propto \exp\left(-\widehat{\text{BIC}}_{\mathcal{M}_k}/2\right)$ and $\sum_{k=1}^K w_{\mathcal{M}_k} = 1$.

6 Numerical comparisons

In this section, we evaluate the performance of the models in Section 4 using our framework.

In the simulation examples, we include three competitive methods for comparison, namely EzGP (Xiao et al., 2021), EEzGP (Xiao et al., 2021), and ctGP (Lin et al., 2024), all of which account for interactions between QQ factors, as discussed in Section 2.2. In the subsequent computer experiment examples, we focus on further investigating the practical performance and interpretability of our proposed methods. The method names represent Gaussian (**Gau**), exponential (**Exp**), and linear (**Linear**) kernels assigned to the latent variables of qualitative variables. The subscripts denote the dimension of the latent variables or indicate the incorporation of ordinal information (**ord**) if it exists. We distinguish between the multiplicative (**multi**) and additive (**add**) relationships between the qualitative variables using superscripts. For example, **Gau**₁^{**multi**} (or respectively **Gau**_{ord}^{**multi**}) represents the multiplicative Gaussian kernel with 1-dimensional (or respectively ordinal) latent variables. To mitigate the risk of local optima, the optimization is initialized from 15 random starting points, and the solution yielding the smallest log-likelihood in (9) is retained. Building on these base models, our model selection and model averaging strategies, as introduced in Section 5, lead to four methods for evaluation: **LOOCV**_{log-lik}, **LOOCV**_{l₂}, **BIC**_{MSel}, and **BIC**_{MAvr}.

Given the hold-out test points $\mathbf{D}^{te} = \{(\mathbf{U}_i^{te}, \mathbf{V}_i^{te})\}_{i=1}^{n_{te}}$, the accuracy is evaluated by the

relative root-mean-squared error (RRMSE), which is defined as

$$\text{RRMSE} = \left\{ \frac{\sum_{i=1}^{n_{te}} (\widehat{Y}(\mathbf{U}_i^{te}, \mathbf{V}_i^{te}) - Y(\mathbf{U}_i^{te}, \mathbf{V}_i^{te}))^2}{\sum_{i=1}^{n_{te}} (Y(\mathbf{U}_i^{te}, \mathbf{V}_i^{te}) - \bar{Y})^2} \right\}^{1/2},$$

where $Y(\mathbf{U}_i^{te}, \mathbf{V}_i^{te})$ and $\widehat{Y}(\mathbf{U}_i^{te}, \mathbf{V}_i^{te})$ denote the true and predicted values at the input $(\mathbf{U}_i^{te}, \mathbf{V}_i^{te})$ and $\bar{Y} = n_{te}^{-1} \sum_{i=1}^{n_{te}} Y(\mathbf{U}_i^{te}, \mathbf{V}_i^{te})$ is the mean of the true responses over the test inputs.

6.1 Simulation examples

Following [Zhang et al. \(2020\)](#), we apply our proposed methods to four real-world engineering models: (i) the beam bending model, (ii) the borehole model, (iii) the output transformerless (OTL) circuit model, and (iv) the piston model. Detailed descriptions of these examples can be found in Section SI.1. In all examples, qualitative variables are generated from quantitative variables, making them ordinal in nature. For a fair comparison, we employ the same dataset consisting of 30 replicates as used in [Zhang et al. \(2020\)](#). For each model, the training points were generated using a maximin Latin hypercube design (LHD) ([Santner et al., 2003](#)), and 10,000 uniformly distributed test points were used for evaluation. Moreover, the results are insensitive to the choice of experimental design, as illustrated by the additional simulation in Supplementary Section SII.1, where random sampling and the MaxPro design ([Joseph et al., 2015, 2020](#)) yield similar performance to the maximin LHD design. The RRMSEs across the 30 replicates are reported in Figure 1. We summarize the key findings below.

Overall, the three competing methods, especially ctGP, tend to yield higher RRMSE values than the methods under our framework. Our methods equipped with different kernels demonstrate varying strengths across the examples. To better showcase the results, we

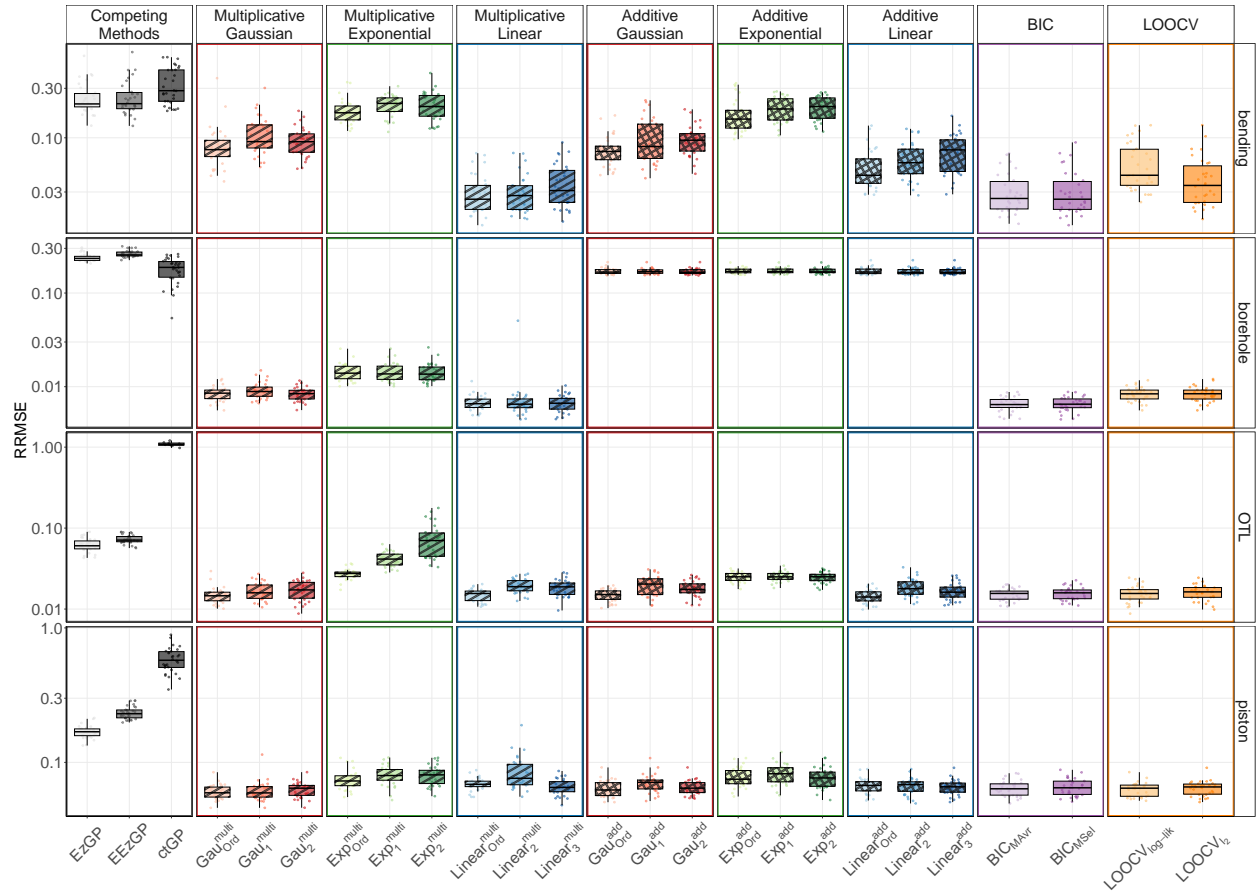


Figure 1: Comparison of RRMSE across different methods and kernel configurations for the beam bending, borehole, OTL circuit, and piston examples. Each boxplot summarizes the results from 30 independent runs with different training sets generated via maximin LHD. All methods were evaluated on the same set of 10,000 uniformly distributed test points.

classify the methods into two categories based on whether they impose additive or multiplicative structures across different qualitative variables. The two classes exhibit distinct performance patterns: (i) the results between the two classes differ significantly in the bore-hole example; (ii) in the OTL example, the differences between Gaussian, exponential, and linear kernels are less pronounced when an additive structure is imposed, compared to a multiplicative structure. Within each class, further comparisons can be made based on the choice of kernel, which determines how the relationships between different levels of each qualitative variable are modeled. Methods using the exponential kernel exhibit poor performance, as reflected by the highest RRMSE values. For the other two kernels, methods with the linear kernel perform better than those with the Gaussian kernel in the beam bending, while the former is slightly worse than the latter. For the borehole and OTL examples, they are comparable. These differences can be attributed to the different correlation structures between qualitative variables in the four examples.

The dimension of the latent vector plays a critical role in determining the performance of methods using the same kernel. For example, in the beam bending example, methods with the linear kernel and a latent vector dimension of $l_j = 2$ ($\text{Linear}_2^{\text{multi}}$ and $\text{Linear}_2^{\text{add}}$) outperform those with $l_j = 3$ ($\text{Linear}_3^{\text{multi}}$ and $\text{Linear}_3^{\text{add}}$). Conversely, in the piston example, the method using the additive Gaussian kernel with $l_j = 2$ ($\text{Gau}_2^{\text{add}}$) achieves better performance compared to its counterpart with $l_j = 1$ ($\text{Gau}_1^{\text{add}}$). These results demonstrate the importance of selecting an appropriate latent vector dimension. When a low-dimensional latent vector is sufficient to capture the structure of the data, increasing the dimension can introduce additional uncertainty, reduce generalizability, and degrade performance. Conversely, an overly low-dimensional vector may fail to capture the essential relationships and structural complexity. Striking the right balance is essential to ensure the model is both accurate and robust and avoid the pitfalls of over-parameterization or under-specification.

In this simulation, incorporating the ordinal nature of qualitative variables, when present, generally leads to improved performance. Traditional GP models with QQ inputs often treat ordinal variables as nominal ones. While this approach is convenient, it fails to fully exploit the inherent ordinal structure within the data. In contrast, our methods, which explicitly account for the ordinal structure, consistently have superior performance. Specifically, $\text{Gau}_{\text{ord}}^{\text{multi}}$, $\text{Gau}_{\text{ord}}^{\text{add}}$, $\text{Exp}_{\text{ord}}^{\text{multi}}$ and $\text{Exp}_{\text{ord}}^{\text{add}}$ in most cases outperform $\text{Gau}_1^{\text{multi}}$, $\text{Gau}_1^{\text{add}}$, $\text{Exp}_1^{\text{multi}}$ and $\text{Exp}_1^{\text{add}}$ across all four examples. Moreover, $\text{Linear}_{\text{ord}}^{\text{multi}}/\text{Linear}_{\text{ord}}^{\text{add}}$ outperforms $\text{Linear}_2^{\text{multi}}/\text{Linear}_2^{\text{add}}$ in the OTL example and performs comparably in the other examples. These findings highlight the limitations of treating ordinal variables as nominal and underscore the importance of leveraging the ordinal structure to enhance modeling accuracy and efficiency.

Now we investigate the reason behind the improved performance when incorporating ordinal information. Figure 2 visualizes the latent vectors estimated by $\text{Gau}_1^{\text{multi}}$, $\text{Gau}_{\text{ord}}^{\text{multi}}$, $\text{Exp}_1^{\text{multi}}$, and $\text{Exp}_{\text{ord}}^{\text{multi}}$ in the OTL example where $\text{Gau}_{\text{ord}}^{\text{multi}}$ and $\text{Exp}_{\text{ord}}^{\text{multi}}$ demonstrate significantly better performance than other two. First, let us focus on the factor R_f . The latent vectors estimated by $\text{Gau}_1^{\text{multi}}$ generally follow the order of the levels, with only one exception. This indicates that when using the Gaussian kernel, the ordinal structure is sufficiently strong and can be effectively learned for R_f in this example. This observation reinforces the rationale for using ordinal information. When the exponential kernel is applied, treating the ordinal variable as nominal (i.e., $\text{Exp}_1^{\text{multi}}$) introduces more noise, as the estimated latent vectors exhibit different ordering patterns across replications. By incorporating ordinal information, $\text{Exp}_{\text{ord}}^{\text{multi}}$ significantly enhances its predictive power. For the additive kernel, the phenomenon is similar and can be found in Supplementary Figure S1. Next, let us examine β , which has six levels and poses a greater challenge. Both $\text{Gau}_1^{\text{multi}}$ and $\text{Exp}_1^{\text{multi}}$ exhibit noisy latent vector estimations. In many replications, most latent vectors corresponding to the six levels estimated by $\text{Exp}_{\text{ord}}^{\text{multi}}$ are identical, which indicates that the different levels of β are

difficult to distinguish using this dataset. In such cases, estimating too many parameters for the latent parameterization may lead to overfitting. By comparing the methods that treat the variable as nominal ($\text{Exp}_1^{\text{multi}}$ and $\text{Gau}_1^{\text{multi}}$) with those that impose an ordinal structure ($\text{Exp}_{\text{ord}}^{\text{multi}}$ and $\text{Gau}_{\text{ord}}^{\text{multi}}$), it becomes clear that incorporating ordinal constraints has the effect of regularizing parameter estimation and hence enhancing generalizability in this case.

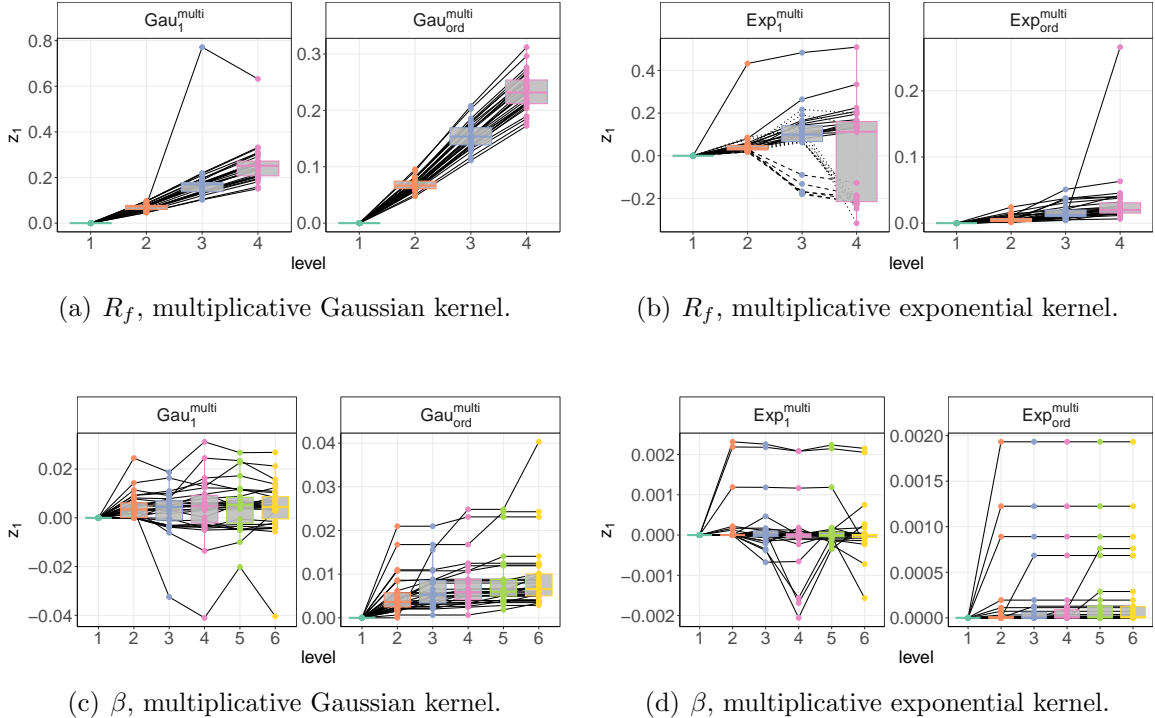


Figure 2: The boxplots and scatter points depict the latent vectors z_1 for resistance R_f and current gain β , estimated by $\text{Gau}_1^{\text{multi}}$, $\text{Gau}_{\text{ord}}^{\text{multi}}$, $\text{Exp}_1^{\text{multi}}$, and $\text{Exp}_{\text{ord}}^{\text{multi}}$, respectively, across 30 replications in the OTL example. Points from the same replication are connected by lines. In the R_f panel for $\text{Exp}_1^{\text{multi}}$, different line types indicate different ordering patterns of the estimated latent vectors: solid lines correspond to replications where the original level order is preserved, dashed lines indicate a reversal between the second and third levels, and dotted lines indicate a swap between the third and fourth levels.

Since assigning different kernels yields varying performance, it is important to select an appropriate one. We compare three model selection strategies (BIC_{MSel} , $\text{LOOCV}_{\text{L}_2}$, and $\text{LOOCV}_{\text{log-lik}}$) and one model averaging strategy (BIC_{MAvr}) proposed in Section 5 through their normalized RRMSE ranks, where a lower rank indicates better (i.e., lower) RRMSE

performance. As shown in Table 3, these strategies perform satisfactorily in general because they always select methods ranked in the top half. For the model selection strategies, $\text{LOOCV}_{\log\text{-lik}}$ achieves relatively stable ranks, which fall within the top 20% to 30%, and shows competitive performance in the OTL and piston examples. In contrast, BIC_{MSel} and BIC_{MAvr} achieve the best performance in the bending and borehole examples, while their performance is less favorable in the piston example. Here, BIC_{MAvr} achieves more stable performance across various scenarios and demonstrates better performance than BIC_{MSel} in both the OTL and piston examples.

Table 3: Normalized rank of RRMSE for BIC_{MAvr} , BIC_{MSel} , $\text{LOOCV}_{\log\text{-lik}}$, and LOOCV_{l_2} across simulation types. The ranks for BIC_{MSel} , $\text{LOOCV}_{\log\text{-lik}}$, and LOOCV_{l_2} are computed among the 18 base models based on ascending RRMSE, whereas the rank for BIC_{MAvr} is determined by including its RRMSE alongside the 18 base models. A lower rank implies a lower RRMSE value. The results are summarized as median, mean, and standard deviation (SD) across replications.

Method	bending			borehole			OTL			piston		
	Median	Mean	SD	Median	Mean	SD	Median	Mean	SD	Median	Mean	SD
BIC_{MAvr}	0.105	0.125	0.040	0.105	0.130	0.047	0.263	0.254	0.136	0.342	0.321	0.211
BIC_{MSel}	0.111	0.119	0.111	0.111	0.113	0.068	0.278	0.285	0.183	0.389	0.398	0.236
$\text{LOOCV}_{\log\text{-lik}}$	0.222	0.248	0.106	0.250	0.237	0.076	0.278	0.280	0.178	0.222	0.302	0.211
LOOCV_{l_2}	0.111	0.157	0.117	0.278	0.246	0.071	0.278	0.296	0.179	0.333	0.370	0.209

To sum up, this simulation study highlights the significance of selecting appropriate kernels, optimizing latent vector dimensions, leveraging ordinal structures, and employing effective model selection or averaging strategies. To further examine the prediction accuracy and computational cost for various dimensions, we conduct additional experiments on the borehole example with different discretization degrees. Our methods achieve the lowest RRMSE in moderate dimension. As an example of our approach, $\text{Gau}_{\text{ord}}^{\text{multi}}$ delivers more accurate predictions than ctGP , EzGP , and EEzGP across all degrees within a reasonable computational time. Interestingly, a trade-off between accuracy and time can be seen. For instance, while ctGP becomes more accurate with finer discretization, its computational

cost increases more rapidly than other methods. Another observation is that $\text{Linear}_{\text{ord}}^{\text{multi}}$ attains higher predictive accuracy than both $\text{Linear}_2^{\text{multi}}$ and $\text{Linear}_1^{\text{multi}}$ at the expense of a higher computational cost. The detailed setups and results are provided in Supplementary Section SII.2.

6.2 A 3D coupled finite element model for embankments

In this section, we apply various methods to a fully 3D coupled finite element model, which has been rigorously validated for its effectiveness in capturing the deformations and stresses of full-scale embankments (Liu and Rowe, 2015). The corresponding computer experiments involve one quantitative factor and three qualitative factors. The quantitative factor $u_1 \in [0, 14]$ (in m) represents the distance from the embankment centerline to the embankment shoulder, taking 29 uniformly spaced values. The three qualitative factors are the embankment construction rate $v_1 \in \{1, 5, 10\}$ (in m/month), the Young's modulus of columns $v_2 \in \{50, 100, 200\}$ (in MPa), and the reinforcement stiffness $v_3 \in \{1578, 4800, 8000\}$ (in kN/m). This example is particularly suitable for studying scenarios with a limited number of levels for qualitative variables, as each qualitative factor here has only three levels.

As described in Deng et al. (2017) and Kang and Deng (2020), for each value of the quantitative factor, a three-level fractional factorial design with nine runs is employed for the qualitative factors, resulting in a total of 261 design points. The test dataset consists of 29 input settings, where u_1 takes 29 equally spaced values over interval $[0, 14]$, and the qualitative factors are fixed at $(v_1, v_2, v_3) = (5, 100, 4800)$. Among the design points, two points $(u_1, v_1, v_2, v_3) \in \{(14, 5, 200, 8000), (14, 10, 200, 1578)\}$ are identified as having potentially reversed labels and are excluded from the training process (see Supplementary Section SI.3 for details). Additionally, training on the entire dataset fails. A plausible explanation is that some points that are too close to each other can cause a near singularity when computing

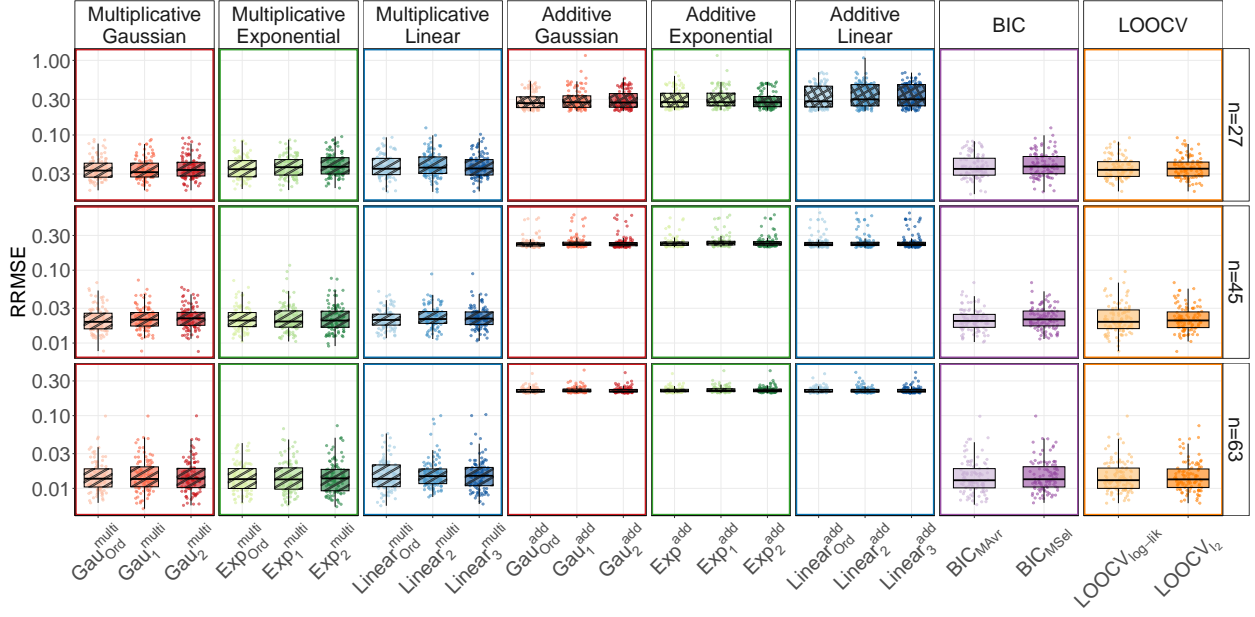


Figure 3: Comparison of RRMSE across different methods and kernel configurations for the 3D coupled finite element model for embankments, evaluated on the remaining points of the training dataset. Each boxplot summarizes results from 100 runs. In each run, the model is trained using a subset of 27, 45, or 63 design points randomly sampled from the training dataset.

\mathbf{R}^{-1} in (9). To address this, subsets of 3, 5, and 7 points are randomly selected at each combination of the qualitative factors, resulting in training sets with 27, 45, and 63 design points, respectively. To evaluate the performance of each method, the RRMSE is calculated using (i) the remaining points in the training dataset and (ii) the independent test dataset.

As shown in Figures 3 and 4, increasing the latent dimension generally improves prediction accuracy. Since the number of levels is relatively low (three), increasing the dimension from one to two for Gaussian and exponential kernels or from two to three for Gaussian kernels only requires estimating one additional parameter, which enhances model flexibility with a slight increase in complexity.

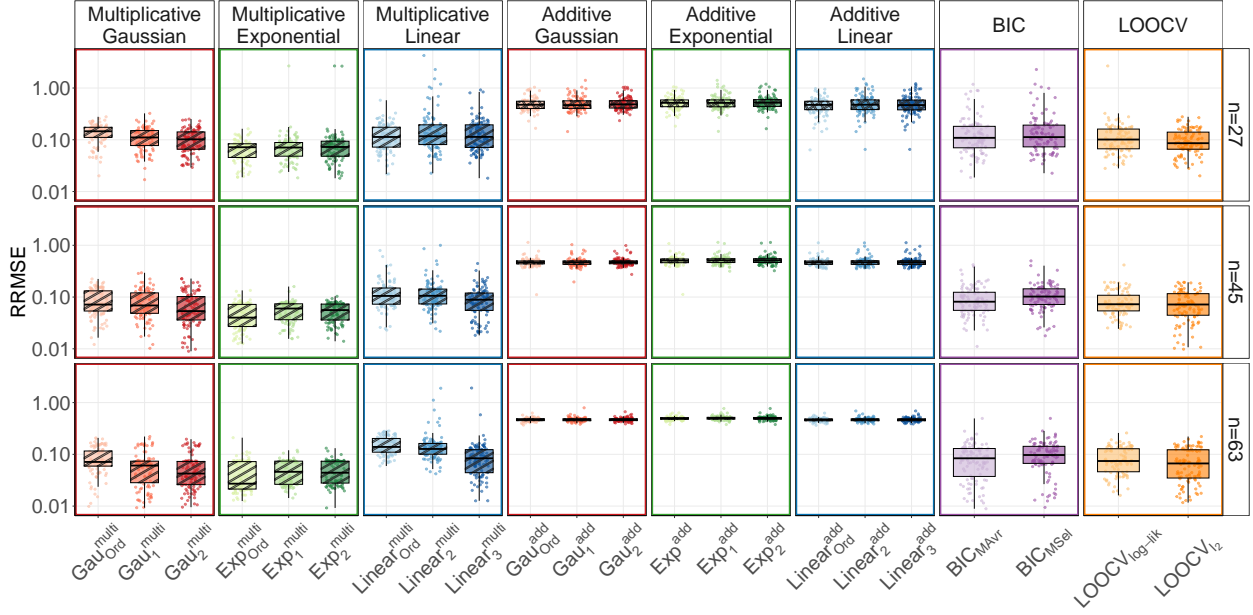


Figure 4: Comparison of RRMSE across different methods and kernel configurations for the 3D coupled finite element model for embankments, evaluated on the independent test dataset. Each boxplot summarizes results from 100 runs. In each run, the model is trained using a subset of 27, 45, or 63 design points randomly sampled from the training dataset.

6.3 A material design example

We then investigate a material design example focusing on the elastic and mechanical properties of materials (Balachandran et al., 2016). The dataset consists of 223 compounds from the M_2AX family, with their elastic properties computed using density functional theory and the planewave/core potential formalism (Cover et al., 2009). The responses include the bulk modulus, shear modulus, and Young's modulus. This example involves three nominal variables, each with multiple levels: the M atom has ten levels {Sc, Ti, V, Cr, Zr, Nb, Mo, Hf, Ta, W}, the A atom has two levels {C, N}, and the X atom has twelve levels {Al, Si, P, S, Ga, Ge, As, Cd, In, Sn, Tl, Pb}. In addition, the M , A , and X atoms are associated with three, two, and two quantitative features, respectively, that describe their physical properties. Using the shear modulus as a response, previous studies have demonstrated the importance of incorporating qualitative variables into the prediction (Zhang et al., 2020).

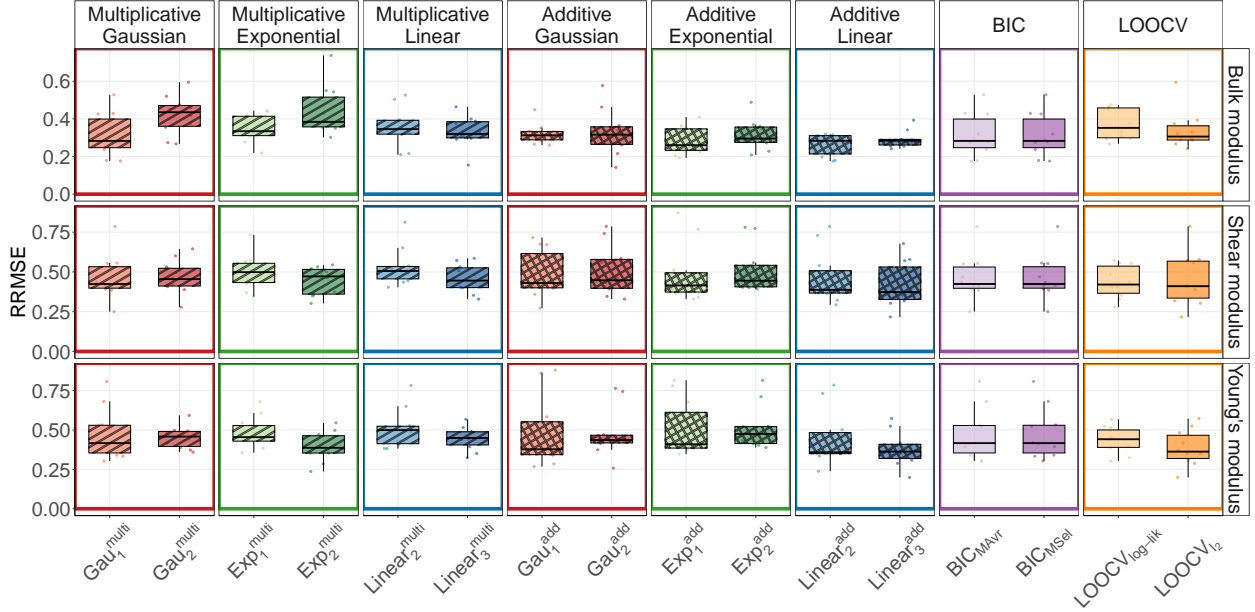


Figure 5: Comparison of RRMSE across different methods and kernel configurations for the material design example. Each boxplot reflects results from 10 resampling runs, where 200 points are used for training and 23 points for testing in each run.

Here, we extend this investigation by comparing the performance of various kernel configurations across all three responses. Following the previous approach, we randomly select 200 data points from a total of 223 as the training set, with the remaining 23 data points reserved for testing. The evaluation is repeated 10 times.

Table 4: Summary of RRMSE for 12 base models, three model selection methods, and one model averaging method. Results are presented as median, mean, and standard deviation (SD) across replications. The smallest RRMSE mean and median values are presented in boldface for each response.

Modulus	Criterion	Method															
		Gau ^{multi}		Exp ^{multi}		Linear ^{multi}		Gau ^{add}		Exp ^{add}		Linear ^{add}		BIC		LOOCV	
		1-d	2-d	1-d	2-d	2-d	3-d	1-d	2-d	1-d	2-d	2-d	3-d	MAvr	MSel	log-lik	l_2
Bulk	Mean	0.314	0.419	0.350	0.441	0.357	0.331	0.320	0.327	0.284	0.315	0.263	0.291	0.314	0.314	0.372	0.339
	Median	0.283	0.435	0.335	0.384	0.345	0.320	0.312	0.316	0.260	0.295	0.284	0.284	0.283	0.283	0.352	0.306
	SD	0.115	0.104	0.075	0.132	0.104	0.083	0.054	0.123	0.073	0.081	0.058	0.045	0.115	0.115	0.083	0.101
Shear	Mean	0.465	0.468	0.499	0.442	0.531	0.457	0.481	0.504	0.486	0.510	0.459	0.418	0.465	0.465	0.437	0.454
	Median	0.424	0.455	0.498	0.472	0.506	0.445	0.430	0.447	0.415	0.445	0.387	0.373	0.424	0.424	0.421	0.410
	SD	0.143	0.106	0.113	0.088	0.120	0.091	0.151	0.160	0.185	0.149	0.170	0.145	0.142	0.143	0.102	0.169
Young	Mean	0.475	0.452	0.482	0.396	0.508	0.446	0.478	0.478	0.501	0.514	0.443	0.377	0.475	0.475	0.435	0.387
	Median	0.416	0.458	0.454	0.387	0.499	0.449	0.377	0.436	0.409	0.475	0.358	0.363	0.416	0.416	0.441	0.363
	SD	0.163	0.071	0.101	0.095	0.126	0.075	0.225	0.157	0.182	0.143	0.179	0.109	0.163	0.163	0.086	0.114

The RRMSEs across ten replicates for the three responses are shown in Figure 5, with a

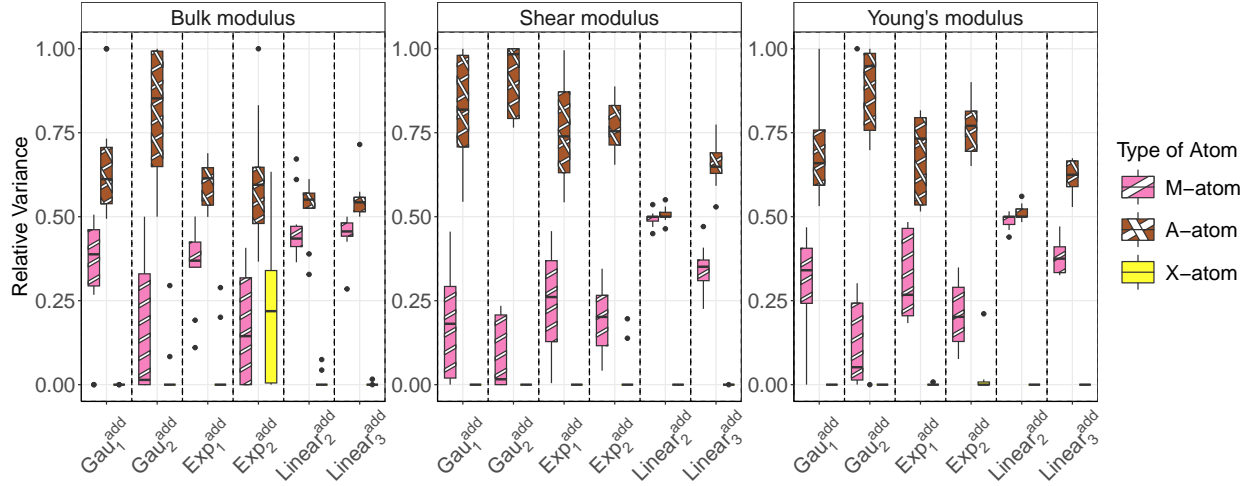


Figure 6: Comparison of relative weights ψ_j defined in (8) for methods with additive kernels in the material design example.

summary provided in Table 4. In this example, either $\text{Linear}_2^{\text{add}}$ or $\text{Linear}_3^{\text{add}}$ generally achieves the lowest mean or median RRMSE, with $\text{Linear}_3^{\text{add}}$ exhibiting lower variation. Assigning either an additive or multiplicative kernel results in comparable performance; however, the additive kernel generally performs slightly better.

To understand this difference, we visualize the relative weights $\{\psi_j\}$ of the additive kernel in Figure 6. Denote the X-atom as the j_0 th qualitative variable. We observe that its relative weights ψ_{j_0} are close to zero, which indicates that the X-atom contributes minimally to the variation in the response. In other words, there is little distinction between different levels of the X-atom. The same effect can also be achieved by using the multiplicative kernel, provided that $\tau_{v,v'}^{j_0} \approx 1$ in (3) for all $v, v' \in \{1, \dots, a_{j_0}\}$, i.e., the correlations between any two levels of the X-atom are approximately one. When the levels are represented via latent variables, this condition says that the latent variables associated with different levels are nearly identical. However, to determine such a structure accurately would require a large amount of data. Consequently, when a qualitative variable has little or no effect on the response, the use of the additive kernel may capture this pattern more effectively.

7 Summary remarks and further discussion

In this paper, we introduce a general framework for modeling QQ factors using GP. The main idea comes from an insightful approach by [Zhang et al. \(2020\)](#), which maps each qualitative factor into a continuous latent space. We realize that this approach includes many existing models as special cases by employing multiplicative or additive structures and by adopting kernel functions—such as Gaussian, exponential, and linear kernels—for the latent vectors of each qualitative variable. We systematically evaluate the performance of these models. Methods with the linear kernel achieve superior performance in certain cases. Overall, models using multiplicative kernels tend to outperform those using additive kernels, except when some qualitative variables are inactive in predicting the response. Moreover, leveraging ordinal information can improve performance. Finally, both model averaging and model selection strategies effectively identify appropriate models and yield satisfactory predictive accuracy.

Using this framework, we establish two important connections that enhance both conceptual understanding and practical implementation. First, our framework bridges the gap between quantitative input-only modeling and QQ input modeling. This connection enables the extension of techniques from quantitative input-only Gaussian processes to situations involving both quantitative and qualitative inputs. A common approach is to transform qualitative levels into dummy variables and then apply kernels designed for quantitative variables. While this method is straightforward to implement, it often complicates the interpretation of learned scale parameters. Beyond the approach taken by [Zhang et al. \(2020\)](#), we take a further step by studying its compatibility with other kernels for quantitative inputs. This can facilitate future work to develop more complex kernels for QQ inputs. However, careful attention must be paid to improve interpretability and tackle computational challenges arising from the discrete nature of qualitative inputs.

Second, we demonstrate that this framework unifies many existing approaches by choosing different kernels, as shown in Section 2.2. For these models, we propose model selection or model averaging procedures, the effectiveness of which is confirmed by the simulation and numerical results in Section 6. Besides unifying existing approaches, we find that assigning a low-dimensional linear kernel is equivalent to imposing a low-rank structure on the correlation matrix across different levels. The effectiveness of low-rank structures has been well demonstrated in many fields, such as economics (Fan et al., 2008), epidemiology (Zhong et al., 2024), and engineering (Chang et al., 2021).

Finally, our framework can easily handle ordinal variables by imposing constraints on the latent vectors to incorporate the ordinal information. To facilitate computation, we transform these constraints into unconstrained forms for the Gaussian and exponential kernels and box constraints for the linear kernel. The advantages of incorporating ordinal information are demonstrated by our simulation results. However, one potential limitation is that we require the latent vector to have length one for the Gaussian and exponential kernels, and length two for the linear kernel, which may affect its generality. For instance, Qian et al. (2008) proposed restricting the correlation to be non-increasing along the ordinal levels, a theoretically rigorous but computationally demanding approach. Further investigation into optimal strategy for incorporating ordinal information is left for future research.

A Proofs of Theorem 1 and Propositions 1 and 2

Proof of Theorem 1. Under the linear kernel, the latent parameterization $\{\mathbf{W}_v\}$ can be obtained through the Cholesky decomposition of the kernel matrix induced by the latent parameterization $\{\mathbf{Z}_v\}$ under the Mercer kernel.

Specifically, let $\mathbf{K}_{\{\mathbf{Z}_v\}}^{(j)}$ denote the kernel matrix of the j th qualitative variable, where the

(v, v') th element is given by $K_j^{\mathbf{Z}}(\mathbf{z}_v^{(j)}, \mathbf{z}_{v'}^{(j)})$ for $v, v' \in \{1, \dots, a_j\}$. The Cholesky decomposition of $\mathbf{K}_{\{\mathbf{Z}_V\}}^{(j)}$ is expressed as $\mathbf{K}_{\{\mathbf{Z}_V\}}^{(j)} = (\mathbf{R}^{(j)})^\top (\mathbf{R}^{(j)})$, where $\mathbf{R}^{(j)} = (\mathbf{r}_1^{(j)}, \mathbf{r}_2^{(j)}, \dots, \mathbf{r}_{a_j}^{(j)})$ is an upper triangular matrix of dimension $a_j \times a_j$. Defining $\mathbf{w}_i^{(j)} = \mathbf{r}_i^{(j)}$ for $i \in \{1, 2, \dots, a_j\}$, we then obtain a latent parameterization such that $K_j^{\mathbf{Z}}(\mathbf{z}_v^{(j)}, \mathbf{z}_{v'}^{(j)}) = K_j^{\mathbf{W}}(\mathbf{w}_v^{(j)}, \mathbf{w}_{v'}^{(j)})$ for all $v, v' \in \{1, \dots, a_j\}$.

Since the structure between different qualitative variables is either multiplicative as in (7) or additive as in (8), the equality $K_{\mathbf{Z}}(\mathbf{Z}_V, \mathbf{Z}_{V'}) = K_{\mathbf{W}}(\mathbf{W}_V, \mathbf{W}_{V'})$ holds for all $\mathbf{V}, \mathbf{V}' \in \times_{j=1}^J \{1, 2, \dots, a_j\}$. \square

Proof of Proposition 1. Proof of (a). Existence. We perform the QR decomposition

$$(\mathbf{z}_1^{(1)}, \mathbf{z}_2^{(1)}, \dots, \mathbf{z}_{l_1}^{(1)}) = \mathbf{Q}\mathbf{R},$$

where $\mathbf{Q} \in \mathbb{R}^{l_1 \times l_1}$ is an orthogonal matrix, and $\mathbf{R} \in \mathbb{R}^{l_1 \times l_1}$ is an upper-triangular matrix with positive diagonal entries. Define

$$(\mathbf{w}_1^{(1)}, \mathbf{w}_2^{(1)}, \dots, \mathbf{w}_{a_1}^{(1)}) := (\mathbf{R}, \mathbf{Q}^\top \mathbf{z}_{l_1+1}^{(1)}, \dots, \mathbf{Q}^\top \mathbf{z}_{a_1}^{(1)}).$$

$\{\mathbf{Z}_V\}$ and $\{\mathbf{W}_V\}$ are equivalent under the linear kernel because they satisfy the desired condition in Lemma S1.

Uniqueness. We have established the existence of such a latent parameterization. According to Lemma S1, any equivalent parameterization satisfies

$$(\mathbf{z}_1^{(1)}, \mathbf{z}_2^{(1)}, \dots, \mathbf{z}_{a_1}^{(1)}) = \mathbf{Q}(\mathbf{w}_1^{(1)}, \dots, \mathbf{w}_{a_1}^{(1)})$$

for some orthogonal matrix $\mathbf{Q} \in \mathbb{R}^{l_1 \times l_1}$. The requirements of \mathbf{W}_V in (a) ensure the uniqueness of the QR decomposition, and consequently $\mathbf{Q}, \mathbf{w}_2^{(1)}, \dots, \mathbf{w}_{l_1}^{(1)}$. The uniqueness of the

remaining vectors is derived by solving the remaining $a_1 - l_1$ columns of (11).

Proof of (b). Cartesian coordinates can be uniquely expressed in hyperspherical coordinates as

$$w_{v,l}^{(1)} = r_v \cos(\theta_{v,l}^{(1)}) \prod_{\iota=1}^{l-1} \sin(\theta_{v,\iota}^{(1)}) \text{ for } 1 \leq l < l_1 - 1 \text{ and } w_{v,l}^{(1)} = r_v \prod_{\iota=1}^l \sin(\theta_{v,\iota}^{(1)}) \text{ for } l = l_1 - 1,$$

where $v \in \{1, \dots, a_1\}$, $0 \leq \theta_{v,l}^{(1)} \leq \pi$ for $1 < l < l_1 - 1$ and $0 \leq \theta_{v,l}^{(1)} \leq 2\pi$ for $l = l_1 - 1$. In the above formula, $r_v = \|\mathbf{w}_v\|_2 = \|\mathbf{z}_v\|_2 = 1$ for $1 \leq v \leq a_1$.

To ensure $w_{v,l}^{(1)} = 0$ for all $l > v$, we require $\theta_{v,l}^{(1)} = 0$ for $l = v$. Additionally, we impose $\theta_{v,l}^{(1)} = 0$ for $l > v$ to preserve the equality. Finally, to ensure $w_{v,v}^{(1)} > 0$ for $1 \leq v \leq l_1$, we require $0 \leq \theta_{v,v-1}^{(1)} \leq \pi$ (rather than less than 2π) for $1 \leq v \leq l_1$. These constraints are exactly the ones as described in (b). \square

Proof of Proposition 2. Existence. First, perform the QR decomposition:

$$(\mathbf{z}_2^{(1)} - \mathbf{z}_1^{(1)}, \dots, \mathbf{z}_{l_1+1}^{(1)} - \mathbf{z}_1^{(1)}) = \mathbf{Q}\mathbf{R},$$

where $\mathbf{Q} \in \mathbb{R}^{l_1 \times l_1}$ is an orthogonal matrix, and $\mathbf{R} \in \mathbb{R}^{l_1 \times l_1}$ is an upper triangular matrix with positive diagonal elements. We then define

$$(\mathbf{w}_1^{(1)}, \mathbf{w}_2^{(1)}, \dots, \mathbf{w}_{a_1}^{(1)}) := (\mathbf{0}, \mathbf{R}, \mathbf{Q}^\top(\mathbf{z}_{l_1+2}^{(1)} - \mathbf{z}_1^{(1)}), \dots, \mathbf{Q}^\top(\mathbf{z}_{a_1}^{(1)} - \mathbf{z}_1^{(1)})).$$

By setting \mathbf{Q} and $\mathbf{w} = -\mathbf{Q}^\top \mathbf{z}_1^{(1)}$, $\{\mathbf{W}_V\}$ satisfies the desired condition stated in Lemma S2. Therefore, $\{\mathbf{Z}_V\}$ and $\{\mathbf{W}_V\}$ are equivalent under the isotropic kernel.

Uniqueness. We have already proved that such a latent parameterization exists. Accord-

ing to Lemma S2, there exist an orthogonal matrix \mathbf{Q} and a vector \mathbf{w} such that

$$(\mathbf{z}_1^{(1)}, \mathbf{z}_2^{(1)}, \dots, \mathbf{z}_{a_1}^{(1)}) = \mathbf{Q}(\mathbf{w}_1^{(1)} - \mathbf{w}, \mathbf{w}_2^{(1)} - \mathbf{w}, \dots, \mathbf{w}_{a_1}^{(1)} - \mathbf{w}). \quad (11)$$

Since $\mathbf{w}_1^{(1)} = \mathbf{0}$, comparing the first columns of the two matrices in (11) gives $\mathbf{w} = -\mathbf{Q}^\top \mathbf{z}_1^{(1)}$.

Then, we have

$$(\mathbf{z}_2^{(1)}, \dots, \mathbf{z}_{l_1+1}^{(1)}) = \mathbf{Q}(\mathbf{w}_2^{(1)} + \mathbf{Q}^\top \mathbf{z}_1^{(1)}, \dots, \mathbf{w}_{l_1+1}^{(1)} + \mathbf{Q}^\top \mathbf{z}_1^{(1)}).$$

Rearranging the above formula yields

$$(\mathbf{z}_2^{(1)} - \mathbf{z}_1^{(1)}, \dots, \mathbf{z}_{l_1+1}^{(1)} - \mathbf{z}_1^{(1)}) = \mathbf{Q}(\mathbf{w}_2^{(1)}, \dots, \mathbf{w}_{l_1+1}^{(1)}),$$

which is precisely the QR decomposition. The uniqueness of \mathbf{Q} , $\mathbf{w}_2^{(1)}, \dots, \mathbf{w}_{l_1+1}^{(1)}$, and \mathbf{w} follows directly from the uniqueness of the QR decomposition, given the requirements for the subdiagonal elements. The uniqueness of the remaining vectors can be derived by solving the remaining $a_1 - l_1$ columns of (11). \square

Disclosure statement

The authors have the following conflicts of interest to declare.

Acknowledgments

The authors thank the three reviewers, the Associate Editor, and the Editor for their valuable comments. Deng's work was completed while she was a postdoctoral researcher at the Chinese University of Hong Kong, Shenzhen.

SUPPLEMENTARY MATERIAL

Supplementary File This file includes additional details and results for the numerical comparisons in Section 6, additional lemmas, and their proofs.

Code This file contains an R package, **MixGP**, which implements our methods and includes the code to reproduce all simulations, figures, and tables.

References

Bach, F. and Jordan, M. (2002), “Learning graphical models with Mercer kernels,” *Advances in Neural Information Processing Systems*, 15.

Bachoc, F., Gamboa, F., Loubes, J.-M., and Venet, N. (2017), “A Gaussian process regression model for distribution inputs,” *IEEE Transactions on Information Theory*, 64, 6620–6637.

Balachandran, P. V., Xue, D., Theiler, J., Hogden, J., and Lookman, T. (2016), “Adaptive strategies for materials design using uncertainties,” *Scientific Reports*, 6, 19660.

Byrd, R. H., Lu, P., Nocedal, J., and Zhu, C. (1995), “A limited memory algorithm for bound constrained optimization,” *SIAM Journal on scientific computing*, 16, 1190–1208.

Carpenter, B., Gelman, A., Hoffman, M. D., Lee, D., Goodrich, B., Betancourt, M., Brubaker, M., Guo, J., Li, P., and Riddell, A. (2017), “Stan: A Probabilistic Programming Language,” *Journal of Statistical Software*, 76, 1–32.

Cerda, P., Varoquaux, G., and Kégl, B. (2018), “Similarity encoding for learning with dirty categorical variables,” *Machine Learning*, 107, 1477–1494.

Chang, Y.-H., Wang, X., Zhang, L., Li, Y., Mak, S., Wu, C.-F. J., and Yang, V. (2021), “Reduced-order modeling for complex flow emulation by common kernel-smoothed proper orthogonal decomposition,” *AIAA Journal*, 59, 3291–3303.

Chen, Z., Mak, S., and Wu, C. F. J. (2024), “A hierarchical expected improvement method for Bayesian optimization,” *Journal of the American Statistical Association*, 119, 1619–1632.

Claeskens, G. and Hjort, N. L. (2008), “Frequentist and Bayesian model averaging,” in *Model Selection and Model Averaging*, Cambridge University Press, Cambridge Series in Statistical and Probabilistic Mathematics, p. 192–226.

Cover, M. F., Warschkow, O., Bilek, M. M. M., and McKenzie, D. R. (2009), “A comprehensive survey of M_2AX phase elastic properties,” *Journal of Physics: Condensed Matter*, 21, 305403.

Deng, X., Lin, C. D., Liu, K. W., and Rowe, R. K. (2017), “Additive Gaussian process for computer models with qualitative and quantitative factors,” *Technometrics*, 59, 283–292.

Dubrule, O. (1983), “Cross validation of kriging in a unique neighborhood,” *Journal of the International Association for Mathematical Geology*, 15, 687–699.

Duvenaud, D. K., Nickisch, H., and Rasmussen, C. (2011), “Additive Gaussian processes,” *Advances in Neural Information Processing Systems*, 24.

Fan, J., Fan, Y., and Lv, J. (2008), “High dimensional covariance matrix estimation using a factor model,” *Journal of Econometrics*, 147, 186–197.

Garrido-Merchán, E. C. and Hernández-Lobato, D. (2020), “Dealing with categorical and integer-valued variables in Bayesian optimization with Gaussian processes,” *Neurocomputing*, 380, 20–35.

Gramacy, R. B. and Lee, H. K. H. (2008), “Bayesian treed Gaussian process models with an application to computer modeling,” *Journal of the American Statistical Association*, 103, 1119–1130.

Hung, Y., Lin, L.-H., and Wu, C. F. J. (2023), “Optimal simulator selection,” *Journal of the*

American Statistical Association, 118, 1264–1271.

Joseph, V. R., Gul, E., and Ba, S. (2015), “Maximum projection designs for computer experiments,” *Biometrika*, 102, 371–380.

— (2020), “Designing computer experiments with multiple types of factors: The MaxPro approach,” *Journal of Quality Technology*, 52, 343–354.

Kang, X. and Deng, X. (2020), “Design and analysis of computer experiments with quantitative and qualitative inputs: A selective review,” *Wiley Interdisciplinary Reviews: Data Mining and Knowledge Discovery*, 10, e1358.

Lange, K. (1999), *Numerical Analysis for Statisticians*, Springer.

Li, Z. and Tan, M. H. Y. (2022), “A Gaussian process emulator based approach for Bayesian calibration of a functional input,” *Technometrics*, 64, 299–311.

Lin, W.-A., Sung, C.-L., and Chen, R.-B. (2024), “Category tree Gaussian process for computer experiments with many-category qualitative factors and application to cooling system design,” *Journal of Quality Technology*, 56, 391–408.

Liu, K.-W. and Rowe, R. K. (2015), “Numerical study of the effects of geosynthetic reinforcement viscosity on behaviour of embankments supported by deep-mixing-method columns,” *Geotextiles and Geomembranes*, 43, 567–578.

Luo, H., Cho, Y., Demmel, J. W., Li, X. S., and Liu, Y. (2024), “Hybrid parameter search and dynamic model selection for mixed-variable Bayesian optimization,” *Journal of Computational and Graphical Statistics*, 33, 855–868.

McMillan, N. J., Sacks, J., Welch, W. J., and Gao, F. (1999), “Analysis of protein activity data by Gaussian stochastic process models,” *Journal of Biopharmaceutical Statistics*, 9, 145–160.

Mercer, J. (1909), “Functions of Positive and Negative Type, and their Connection with the

Theory of Integral Equations," *Philosophical Transactions of the Royal Society of London. Series A, Containing Papers of a Mathematical or Physical Character*, 209, 415–446.

Oune, N. and Bostanabad, R. (2021), "Latent map Gaussian processes for mixed variable metamodeling," *Computer Methods in Applied Mechanics and Engineering*, 387, 114128.

Peng, C.-Y. and Wu, C. J. (2014), "On the choice of nugget in kriging modeling for deterministic computer experiments," *Journal of Computational and Graphical Statistics*, 23, 151–168.

Pinheiro, J. C. and Bates, D. M. (1996), "Unconstrained parametrizations for variance-covariance matrices," *Statistics and Computing*, 6, 289–296.

Plate, T. A. (1999), "Accuracy versus interpretability in flexible modeling: Implementing a tradeoff using Gaussian process models," *Behaviormetrika*, 26, 29–50.

Qian, P. Z. G., Wu, H., and Wu, C. J. (2008), "Gaussian process models for computer experiments with qualitative and quantitative factors," *Technometrics*, 50, 383–396.

Rasmussen, C. and Williams, C. (2006), "Model selection and adaptation of hyperparameters," in *Gaussian Processes for Machine Learning*, MIT Press, pp. 105–128.

Rojo-Álvarez, J., Martínez-Ramón, M., Muñoz-Marí, J., and Camps-Valls, G. (2018), "Kernel functions and reproducing kernel Hilbert spaces," in *Digital Signal Processing with Kernel Methods*, John Wiley & Sons, pp. 165–207.

Roustant, O., Padonou, E., Deville, Y., Clément, A., Perrin, G., Giorla, J., and Wynn, H. (2020), "Group kernels for Gaussian process metamodels with categorical inputs," *SIAM/ASA Journal on Uncertainty Quantification*, 8, 775–806.

Santner, T. J., Williams, B. J., Notz, W. I., and Williams, B. J. (2003), *The Design and Analysis of Computer Experiments*, vol. 1, Springer.

Saves, P., Diouane, Y., Bartoli, N., Lefebvre, T., and Morlier, J. (2023), "A mixed-categorical

correlation kernel for Gaussian process,” *Neurocomputing*, 550, 126472.

Schmidt, R. R., Cruz, E. E., and Iyengar, M. (2005), “Challenges of data center thermal management,” *IBM Journal of Research and Development*, 49, 709–723.

Schwarz, G. (1978), “Estimating the dimension of a model,” *The Annals of Statistics*, 461–464.

Tao, S., Apley, D. W., Plumlee, M., and Chen, W. (2021), “Latent variable Gaussian process models: A rank-based analysis and an alternative approach,” *International Journal for Numerical Methods in Engineering*, 122, 4007–4026.

Xiao, Q., Mandal, A., Lin, C. D., and Deng, X. (2021), “EZGP: Easy-to-interpret Gaussian process models for computer experiments with both quantitative and qualitative factors,” *SIAM/ASA Journal on Uncertainty Quantification*, 9, 333–353.

Yerramilli, S., Iyer, A., Chen, W., and Apley, D. W. (2023), “Fully Bayesian inference for latent variable Gaussian process models,” *SIAM/ASA Journal on Uncertainty Quantification*, 11, 1357–1381.

Zhang, Y., Tao, S., Chen, W., and Apley, D. W. (2020), “A latent variable approach to Gaussian process modeling with qualitative and quantitative factors,” *Technometrics*, 62, 291–302.

Zhong, Y., He, K., and Li, G. (2024), “Reduced-rank clustered coefficient regression for addressing multicollinearity in heterogeneous coefficient estimation,” *Biometrics*, 80, ujae076.

Zhou, Q., Qian, P. Z. G., and Zhou, S. (2011), “A simple approach to emulation for computer models with qualitative and quantitative factors,” *Technometrics*, 53, 266–273.

Supplementary Material for “A General Framework For Modeling Gaussian Process with Qualitative and Quantitative Factors”

Linsui Deng and C. F. Jeff Wu

School of Data Science, The Chinese University of Hong Kong, Shenzhen,
China

February 19, 2026

Our supplement is organized as follows. Section [SI](#) provides additional details on the numerical studies, including the simulation settings for benchmark examples and supplementary results for the OTL circuit example, as well as a diagnostic analysis of erroneous inputs in the 3D finite element model. Section [SII](#) presents additional simulation comparisons, including comparisons of different experimental designs and an extensive study of the borehole example under varying discretization levels, with detailed results on prediction accuracy and computational efficiency. Section [SIII](#) contains the technical lemmas and their proofs that support the theoretical results in the main paper. The R package and reproducible code for this work are also available at <https://github.com/denglinsui/MixGP> and <https://github.com/denglinsui/MixGP-manuscript-sourcecode>, respectively.

SI Additional details and results of numerical comparisons

SI.1 Functions used in simulation examples

In the numerical experiments, we adopt the same setting as presented in [Zhang et al. \(2020\)](#). We detail the configurations here for completeness and clarity. Four benchmark examples are considered in this study: *beam bending*, *borehole*, *OTL circuit*, and *piston*. These examples are commonly used for evaluating the performance of surrogate modeling techniques because they are derived from real-world engineering problems and carry significant practical relevance. The functional forms of these four examples are originally defined based on continuous input variables. To adapt them to our study, we discretize certain continuous variables and treat them as ordinal qualitative variables.

The *beam bending* example models the deflection of a beam with an elastic modulus of $E = 600$ GPa. The beam is fixed at one end, with a vertical force of $P = 600$ N applied at the free end. The deflection at the free end depends on the beam length $L \in [10, 20]$, the height of the beam’s cross-section $h \in [1, 2]$, and the cross-sectional shape v , and is given by:

$$y(L, h, v) = \frac{L^3}{3 \times 10^9 h^4 I(v)},$$

where $I(v)$ represents the normalized moment of inertia depending on the cross-section type. In this example, six cross-section types are considered, including circular, square, I-shape, hollow square, hollow circular and H-shape, and the corresponding $I(v)$ are approximately 0.0491, 0.0833, 0.0449, 0.0633, 0.0373, and 0.0167 respectively. The geometric pictures can be found in [Zhang et al. \(2020\)](#).

The *borehole* example considers the flow of water through a borehole that is drilled from the ground surface through two aquifers ([Harper and Gupta, 1983](#); [Morris et al., 1993](#)). The flow rate (in m^3/year) through the borehole is given by:

$$y(r_w, r, T_u, H_u, T_l, H_l, L, K_w) = \frac{2\pi T_u (H_u - H_l)}{\log(r/r_w) \left\{ 1 + \frac{2LT_u}{\log(r/r_w)r_w^2 K_w} + \frac{T_u}{T_l} \right\}},$$

where $r_w \in [0.05, 0.15]$ (in m) is the radius of the borehole, $r \in [100, 50000]$ (in m) is the radius of influence, $T_u \in [63070, 115600]$ (in m^2/year) is the transmissivity of the upper aquifer, $H_u \in [990, 1110]$ (in m) is the potentiometric head of the upper aquifer, $T_l \in [63.1, 116]$ (in m^2/year) is the transmissivity of the lower aquifer, $H_l \in [700, 820]$ (in m) is the potentiometric head of the lower aquifer, $L \in [1120, 1680]$ (in m) is the length of the borehole, and $K_w \in [9855, 12045]$ (in m/year) is the hydraulic conductivity of the borehole lining.

Following [Zhang et al. \(2020\)](#), we adapt this function to evaluate surrogate models with mixed inputs by treating r_w (radius of the borehole) and H_l (potentiometric head of the lower aquifer) as qualitative factors. Specifically, r_w is discretized into three levels $\{0.05, 0.10, 0.15\}$, and H_l is discretized into four levels $\{700, 740, 780, 820\}$.

The *output transformerless (OTL) circuit* example considers the midpoint voltage of a push-pull output transformerless amplifier circuit. This circuit is commonly used in electrical engineering to drive loads without the need for a transformer ([Ben-Ari and Steinberg, 2007](#)). The midpoint voltage (in volts) is modeled as:

$$y(R_{b1}, R_{b2}, R_f, R_{c1}, R_{c2}, B) = \frac{\beta(V_{b1} + 0.74)(R_{c2} + 9)}{\beta(R_{c2} + 9) + R_f} + \frac{11.35R_f}{\beta(R_{c2} + 9) + R_f} + \frac{0.74\beta R_f(R_{c2} + 9)}{R_{c1}\{\beta(R_{c2} + 9) + R_f\}},$$

where $V_{b1} = 12R_{b2}/(R_{b1} + R_{b2})$, $R_{b1} \in [50, 150]$ (in $k\Omega$) is the resistance $b1$, $R_{b2} \in [25, 70]$ (in $k\Omega$) is the resistance $b2$, $R_f \in [0.5, 3]$ (in $k\Omega$) is the resistance f , $R_{c1} \in [1.2, 2.5]$ (in $k\Omega$) is the resistance $c1$, $R_{c2} \in [0.25, 1.2]$ (in $k\Omega$) is the resistance $c2$, and $\beta \in [50, 300]$ (Amperes) is the current gain of the transistor.

Following [Zhang et al. \(2020\)](#), we adapt this example to evaluate surrogate models with mixed inputs by treating R_f (resistance f) and β (current gain) as qualitative factors. Specifically, R_f is discretized into four levels $\{0.5, 1.2, 2.1, 2.9\}$, and β is discretized into six levels $\{50, 100, 150, 200, 250, 300\}$.

The *piston* example models the cycle time of a piston moving within a cylinder. This example simulates the linear motion of a piston being transformed into rotational motion via a connected rod and disk. The cycle time (in seconds) is a measure of the piston's performance and is affected by multiple physical factors. The response function for the cycle time is given by

$$y(M, S, V_0, k, P_0, T_a, T_0) = 2\pi \sqrt{\frac{M}{k + S^2 \frac{P_0 V_0 T_a}{V^2 T_0}}}, \quad (\text{S1})$$

where

$$V = \frac{S}{2k} \sqrt{A^2 + 4k \frac{P_0 V_0}{T_0} T_a - A} \quad \text{and} \quad A = P_0 S + 19.62M - \frac{k V_0}{S}, \quad (\text{S2})$$

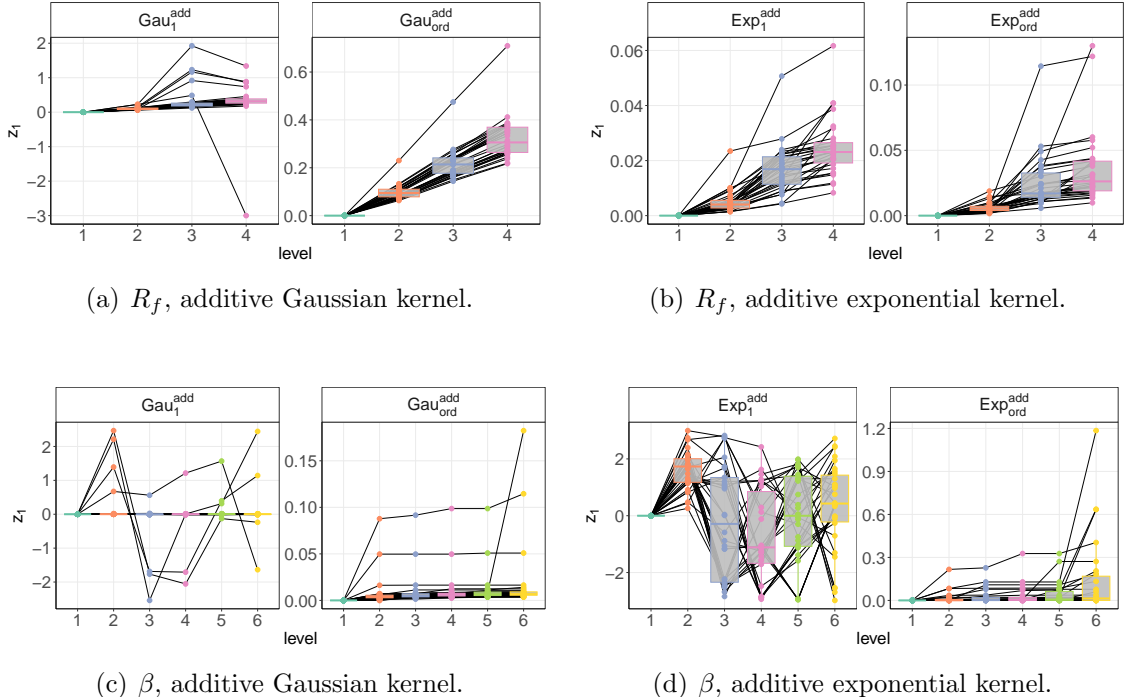


Figure S1: The boxplots and scatter points depict the latent vectors z_1 for resistance R_f and current gain β , estimated by Gau_1^{add} , Gau^{add}_ord , Exp_1^{add} , and Exp_ord^{add} , respectively, across 30 replications in the OTL example. Points from the same replication are connected by lines.

$M \in [30, 60]$ (in kg) represents the mass of the piston, $S \in [0.005, 0.020]$ (in m^2) represents the surface area of the piston, $V_0 \in [0.002, 0.010]$ (in m^3) is the initial gas volume, $k \in [1000, 5000]$ (in N/m) is the spring coefficient, $P_0 \in [90000, 110000]$ (in N/m^2) is the atmospheric pressure, $T_a \in [290, 296]$ (in K) is the ambient temperature, and $T_0 \in [340, 360]$ (in K) is the filling gas temperature.

Following [Zhang et al. \(2020\)](#), this example is adapted to evaluate surrogate models with mixed inputs by treating P_0 (atmospheric pressure) and k (spring coefficient) as qualitative factors. Specifically, P_0 is discretized into three levels $\{90000, 100000, 110000\}$, and k is discretized into five levels $\{1000, 2000, 3000, 4000, 5000\}$.

SI.2 Additional results of the OTL examples

Figure S1 visualizes the latent vectors z_1 for resistance R_f and current gain β , estimated by Gau_1^{add} , Gau^{add}_ord , Exp_1^{add} , and Exp_ord^{add} , respectively, across 30 replications in the OTL example. Similar to Figure 2 in the paper, incorporating ordinal information preserves the natural ordinal structure and benefits from regularization effects.

SI.3 Diagnosis of erroneous inputs in the 3D finite element model

In Section 6.2 of our main paper, we point out two data points, $(u_1, v_1, v_2, v_3) \in \{(14, 5, 200, 8000), (14, 10, 200, 1578)\}$, potentially having reversed labels and exclude them from the training process. Based on the fact that there are only 13 valid combinations for $(v_1, v_2, v_3) \in \{(1, 100, 4800),$

$(5, 200, 1578)\}$, we suspect the correct inputs should be $(u_1, v_1, v_2, v_3) \in \{(14, 1, 100, 4800), (14, 5, 200, 1578)\}$.

To verify our suspicion, we use the 18 base models trained in Section 6.2 to make predictions for both the original inputs— $(14, 5, 200, 8000)$ (Location 1) and $(14, 10, 200, 1578)$ (Location 2)—and the revised inputs— $(14, 1, 100, 4800)$ (Location 1) and $(14, 5, 200, 1578)$ (Location 2). The predicted values are summarized in Table S1.

The observed value at Location 1 is -0.535 , and at Location 2, it is -0.768 . We find that the predictions by using the revised inputs are much closer to the observed values compared to those by using the original inputs. This confirms that the two points are indeed outliers and should be excluded from the training process.

Table S1: Predicted values from 18 base models for both the original and revised inputs at two locations identified as potential outliers. Results are summarized as the median, mean, and standard deviation (SD) across replications.

n	Criterion	Method																	
		Gau ^{multi}			Exp ^{multi}			Linear ^{multi}			Gau ^{add}			Exp ^{add}			Linear ^{add}		
		1-d	2-d	ord	1-d	2-d	ord	1-d	2-d	ord	1-d	2-d	ord	1-d	2-d	ord	1-d	2-d	ord
Location 1 (Original Input)																			
27	Mean	-0.756	-0.756	-0.747	-0.750	-0.748	-0.751	-0.742	-0.744	-0.748	-0.727	-0.721	-0.721	-0.738	-0.732	-0.730	-0.732	-0.732	-0.731
27	Median	-0.754	-0.754	-0.749	-0.754	-0.755	-0.754	-0.746	-0.749	-0.750	-0.729	-0.725	-0.725	-0.742	-0.737	-0.738	-0.731	-0.735	-0.734
27	SD	0.017	0.015	0.010	0.026	0.034	0.010	0.038	0.028	0.011	0.047	0.048	0.042	0.051	0.050	0.045	0.063	0.061	0.052
45	Mean	-0.752	-0.753	-0.748	-0.749	-0.749	-0.750	-0.750	-0.754	-0.751	-0.722	-0.719	-0.717	-0.731	-0.728	-0.726	-0.723	-0.722	-0.721
45	Median	-0.751	-0.753	-0.749	-0.752	-0.752	-0.755	-0.752	-0.754	-0.752	-0.718	-0.717	-0.716	-0.730	-0.726	-0.726	-0.718	-0.718	-0.717
45	SD	0.010	0.009	0.007	0.010	0.009	0.009	0.033	0.010	0.008	0.032	0.032	0.024	0.031	0.031	0.028	0.038	0.037	0.033
63	Mean	-0.752	-0.754	-0.750	-0.750	-0.750	-0.752	-0.752	-0.757	-0.754	-0.711	-0.708	-0.709	-0.718	-0.716	-0.714	-0.709	-0.709	-0.709
63	Median	-0.750	-0.755	-0.750	-0.753	-0.754	-0.756	-0.753	-0.756	-0.755	-0.709	-0.708	-0.708	-0.715	-0.713	-0.713	-0.709	-0.709	-0.709
63	SD	0.008	0.008	0.005	0.009	0.009	0.009	0.030	0.025	0.006	0.017	0.016	0.021	0.020	0.018	0.016	0.016	0.016	0.015
Location 1 (Revised Input)																			
27	Mean	-0.531	-0.531	-0.533	-0.536	-0.536	-0.533	-0.531	-0.533	-0.533	-0.578	-0.575	-0.575	-0.595	-0.587	-0.584	-0.597	-0.595	-0.594
27	Median	-0.533	-0.533	-0.534	-0.535	-0.536	-0.534	-0.534	-0.534	-0.534	-0.559	-0.558	-0.559	-0.575	-0.567	-0.567	-0.564	-0.566	-0.560
27	SD	0.007	0.008	0.007	0.007	0.007	0.006	0.011	0.007	0.008	0.064	0.060	0.056	0.069	0.061	0.055	0.090	0.084	0.088
45	Mean	-0.534	-0.535	-0.535	-0.537	-0.537	-0.536	-0.535	-0.536	-0.535	-0.577	-0.577	-0.572	-0.586	-0.583	-0.581	-0.578	-0.580	-0.576
45	Median	-0.535	-0.535	-0.535	-0.536	-0.536	-0.535	-0.535	-0.535	-0.535	-0.559	-0.554	-0.555	-0.570	-0.563	-0.563	-0.559	-0.559	-0.560
45	SD	0.005	0.005	0.007	0.004	0.004	0.004	0.007	0.006	0.007	0.064	0.066	0.058	0.061	0.063	0.061	0.066	0.064	0.059
63	Mean	-0.536	-0.536	-0.536	-0.536	-0.536	-0.537	-0.537	-0.537	-0.537	-0.552	-0.552	-0.550	-0.551	-0.558	-0.556	-0.554	-0.554	-0.554
63	Median	-0.536	-0.536	-0.536	-0.536	-0.536	-0.536	-0.536	-0.536	-0.537	-0.550	-0.549	-0.550	-0.557	-0.554	-0.555	-0.552	-0.552	-0.551
63	SD	0.002	0.002	0.003	0.002	0.002	0.002	0.004	0.003	0.005	0.019	0.017	0.016	0.020	0.019	0.017	0.017	0.017	0.017
Location 2 (Original Input)																			
27	Mean	-0.841	-0.841	-0.829	-0.841	-0.841	-0.843	-0.811	-0.822	-0.820	-0.882	-0.881	-0.881	-0.880	-0.881	-0.879	-0.877	-0.877	-0.878
27	Median	-0.841	-0.839	-0.833	-0.838	-0.838	-0.838	-0.828	-0.830	-0.827	-0.876	-0.878	-0.877	-0.876	-0.879	-0.874	-0.876	-0.876	-0.871
27	SD	0.028	0.026	0.028	0.019	0.020	0.017	0.058	0.035	0.029	0.051	0.052	0.048	0.050	0.051	0.051	0.062	0.063	0.058
45	Mean	-0.818	-0.823	-0.802	-0.832	-0.830	-0.834	-0.812	-0.821	-0.803	-0.883	-0.884	-0.883	-0.882	-0.884	-0.883	-0.883	-0.883	-0.883
45	Median	-0.827	-0.831	-0.788	-0.833	-0.832	-0.836	-0.817	-0.823	-0.816	-0.876	-0.877	-0.876	-0.876	-0.875	-0.876	-0.874	-0.874	-0.874
45	SD	0.029	0.027	0.027	0.015	0.015	0.013	0.030	0.023	0.035	0.035	0.033	0.032	0.037	0.035	0.036	0.040	0.040	0.039
63	Mean	-0.808	-0.821	-0.799	-0.831	-0.831	-0.834	-0.820	-0.826	-0.822	-0.879	-0.878	-0.878	-0.877	-0.878	-0.878	-0.878	-0.878	-0.878
63	Median	-0.811	-0.835	-0.790	-0.835	-0.834	-0.837	-0.819	-0.829	-0.827	-0.876	-0.876	-0.875	-0.874	-0.876	-0.876	-0.875	-0.875	-0.875
63	SD	0.031	0.029	0.028	0.013	0.014	0.010	0.033	0.027	0.022	0.027	0.026	0.026	0.028	0.027	0.027	0.026	0.026	0.026
Location 2 (Revised Input)																			
27	Mean	-0.773	-0.773	-0.773	-0.775	-0.775	-0.775	-0.775	-0.774	-0.772	-0.826	-0.821	-0.822	-0.827	-0.825	-0.823	-0.817	-0.817	-0.819
27	Median	-0.769	-0.769	-0.769	-0.770	-0.769	-0.770	-0.770	-0.768	-0.768	-0.821	-0.814	-0.817	-0.825	-0.825	-0.823	-0.814	-0.814	-0.813
27	SD	0.015	0.016	0.015	0.017	0.020	0.015	0.017	0.017	0.015	0.049	0.048	0.044	0.049	0.048	0.050	0.059	0.059	0.056
45	Mean	-0.768	-0.768	-0.768	-0.769	-0.768	-0.769	-0.766	-0.765	-0.765	-0.822	-0.821	-0.821	-0.825	-0.825	-0.824	-0.820	-0.818	-0.819
45	Median	-0.766	-0.766	-0.766	-0.766	-0.767	-0.766	-0.765	-0.765	-0.765	-0.817	-0.815	-0.817	-0.819	-0.818	-0.818	-0.813	-0.812	-0.813
45	SD	0.010	0.010	0.009	0.013	0.014	0.011	0.012	0.010	0.006	0.034	0.033	0.031	0.036	0.033	0.039	0.040	0.039	0.039
63	Mean	-0.767	-0.766	-0.766	-0.766	-0.766	-0.768	-0.766	-0.766	-0.766	-0.818	-0.816	-0.816	-0.821	-0.819	-0.818	-0.815	-0.815	-0.814
63	Median	-0.768	-0.769	-0.768	-0.769	-0.769	-0.768	-0.767	-0.769	-0.768	-0.816	-0.813	-0.813	-0.819	-0.818	-0.818	-0.811	-0.811	-0.811
63	SD	0.012	0.012	0.012	0.011	0.012	0.007	0.008	0.012	0.009	0.026	0.025	0.025	0.029	0.027	0.025	0.026	0.026	0.025

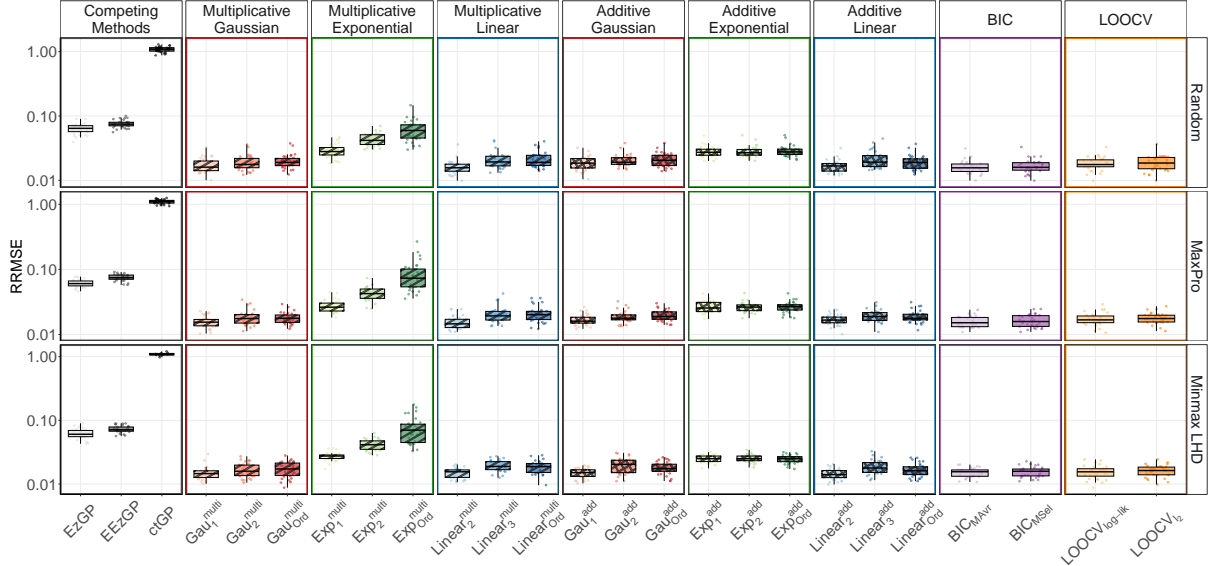


Figure S2: Comparison of RRMSE across different methods and kernel configurations for the OTL circuit example. Each boxplot summarizes the results from 30 independent runs with different training sets generated via minimax LHS, random, and MaxPro designs, respectively. All methods were evaluated on the same set of 10,000 uniformly distributed test points.

SII Additional simulation comparisons

SII.1 Comparisons of different experimental designs

In this section, we examine the effect of experimental design on model performance. Specifically, we consider random sampling, the MaxPro design (Joseph et al., 2015, 2020), and the maximin Latin hypercube design (LHD) (Santner et al., 2003), which was previously examined in Section 6.1, each using 80 training points. As shown in Figure S2, the RRMSE values are highly consistent across all three designs for every method, indicating that the choice of design has a negligible impact on performance.

SII.2 The borehole example with varying discretization degree

In this section, we evaluate the predictive accuracy and computational efficiency of various methods for the borehole example under different discretization levels.

In the preliminary example presented in Section 6.1, r_w was discretized into $q_1 = 3$ levels and H_l into $q_2 = 4$ levels. Here, we extend our analysis by considering multiple combinations of discretization degrees: $q_1 \in \{2, 4, 6\}$ for r_w and $q_2 \in \{2, 4, 6, 8, 10\}$ for H_l . We generate $5q_1q_2$ design points using a minimax LHD, and map $r_w \in [0.05, 0.15]$ and $H_l \in [700, 820]$ to equally spaced values. To save computation time, we run our methods with only three random restarts and select the solution yielding the smallest log-likelihood.

Figures S3–S5 report the RRMSEs of all methods. Consistent with the results in Section 6.1, methods with additive kernels (including the competing methods EzGP and EEzGP) exhibit poor predictive performance. Methods with multiplicative Gaussian and exponential kernels generally perform well. In contrast, methods with multiplicative linear kernels deliver satisfactory results only under very coarse discretization ($q_1 = 2, q_2 = 2$) if ordinal information is not leveraged, possibly because fewer restarts increase the risk of getting stuck in local optima. By

comparison, $\text{Linear}_{\text{ord}}^{\text{multi}}$, together with $\text{Gau}_{\text{ord}}^{\text{multi}}$, generally exhibits the best performance, which indicates that incorporating ordinal information can substantially enhance predictive accuracy and also improve optimization stability.

Table S2 summarizes the computational times of three competing methods and our 18 base methods. The computational time of model selection and model averaging approaches are not reported, as they are constructed by post-processing and aggregating the results from our base models, rather than being standalone methods with minimal additional computational costs. All computational times were measured on a personal computer equipped with a 13th Gen Intel(R) Core(TM) i7-13700KF CPU (3.40 GHz), 64 GB RAM, running Windows 10 and R 4.4.1. EEzGP is the fastest overall. ctGP is efficient when the number of discretization levels is small, but its computational time increases rapidly as the levels grow. EzGP has complexity comparable to that of our base methods. For the base methods, computational time generally increases with latent dimension. With Gaussian or exponential kernels, methods incorporating ordinal information ($\text{Gau}_{\text{ord}}^{\text{multi}}$, $\text{Gau}_{\text{ord}}^{\text{add}}$, $\text{Exp}_{\text{ord}}^{\text{multi}}$, and $\text{Exp}_{\text{ord}}^{\text{add}}$) exhibit computational time comparable to the corresponding methods with the same latent dimension $l_j = 1$ ($\text{Gau}_1^{\text{multi}}$, $\text{Gau}_1^{\text{add}}$, $\text{Exp}_1^{\text{multi}}$, and $\text{Exp}_1^{\text{add}}$), and can even be faster when the discretization degree is high. However, with multiplicative linear kernels, incorporating ordinal information greatly increases costs. Despite the higher computational time, $\text{Linear}_{\text{ord}}^{\text{multi}}$ achieves higher prediction accuracy than $\text{Linear}_2^{\text{multi}}$ or $\text{Linear}_1^{\text{multi}}$. Thus, there is a trade-off between accuracy and efficiency.

Figure S6 displays the RRMSE and computational time trends of EzGP, EEzGP, ctGP, $\text{Gau}_{\text{ord}}^{\text{multi}}$, $\text{Linear}_{\text{ord}}^{\text{multi}}$, and $\text{Linear}_2^{\text{multi}}$. Among our methods, $\text{Linear}_{\text{ord}}^{\text{multi}}$ and $\text{Linear}_2^{\text{multi}}$ represent the slowest and fastest in terms of computational time, respectively; from the perspective of prediction accuracy, $\text{Gau}_{\text{ord}}^{\text{multi}}$ consistently ranks among the top-performing base methods; and we include BIC_{MAvr} as an exemplar of the four model averaging and model selection methods because they yield similar predictive accuracy in the reported RRMSE results. EzGP is the fastest method, but the predictive accuracy of EzGP and EEzGP is relatively low. Although finer discretization requires estimating correlations among more levels, the RRMSE of ctGP decreases as larger sample sizes offset the added complexity. This gain in accuracy comes at the cost of reduced computational efficiency. For our methods, RRMSE decreases at low to moderate discretization degrees and increases when the degree is high. Finally, $\text{Gau}_{\text{ord}}^{\text{multi}}$ delivers high predictive accuracy while maintaining reasonable computational time.

SIII Technical lemmas and their proofs

In this section, we demonstrate the parametric equivalence under the conditions $I = 0$, $J = 1$, and when the two kernels $K_{\mathbf{Z}}(\cdot, \cdot)$ and $K_{\mathbf{W}}(\cdot, \cdot)$ are identical. Under these assumptions, the equivalence of parameterizations depends solely on the latent parameterizations $\{\mathbf{Z}_V\}$ and $\{\mathbf{W}_V\}$.

For the linear kernel, Lemma S1 states that the equivalence of the latent parameterizations is determined up to an orthogonal transformation.

Lemma S1 (Equivalence under Linear Kernel). *Two latent parameterizations $\{\mathbf{W}_V\}$ and $\{\mathbf{Z}_V\}$ are equivalent under the linear kernel if and only if $(\mathbf{z}_1^{(1)}, \mathbf{z}_2^{(1)}, \dots, \mathbf{z}_{a_1}^{(1)}) = \mathbf{Q}(\mathbf{w}_1^{(1)}, \mathbf{w}_2^{(1)}, \dots, \mathbf{w}_{a_1}^{(1)})$ for some orthogonal matrix $\mathbf{Q} \in \mathbb{R}^{l_1 \times l_1}$ such that $\mathbf{Q}^\top \mathbf{Q} = \mathbf{I}_{l_1 \times l_1}$.*

Proof of Lemma S1. Denote $\mathbf{Z}^{(1)} = (\mathbf{z}_1^{(1)}, \mathbf{z}_2^{(1)}, \dots, \mathbf{z}_{a_1}^{(1)})$ and $\mathbf{W}^{(1)} = (\mathbf{w}_1^{(1)}, \mathbf{w}_2^{(1)}, \dots, \mathbf{w}_{a_1}^{(1)})$. If there exists an orthogonal matrix $\mathbf{Q} \in \mathbb{R}^{l_1 \times l_1}$ such that $\mathbf{Z}^{(1)} = \mathbf{Q}\mathbf{W}^{(1)}$, then we have

$$(\mathbf{W}^{(1)})^\top \mathbf{W}^{(1)} = (\mathbf{W}^{(1)})^\top \mathbf{Q}^\top \mathbf{Q} \mathbf{W}^{(1)} = (\mathbf{Z}^{(1)})^\top \mathbf{Z}^{(1)},$$

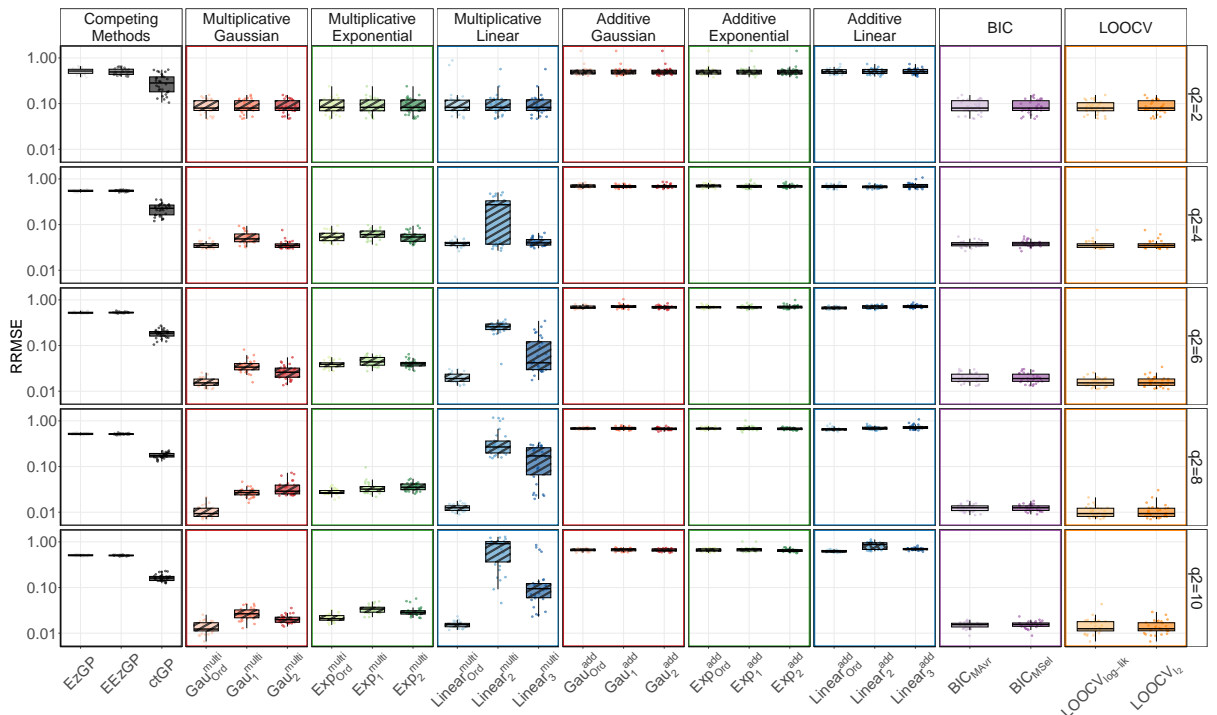


Figure S3: Comparison of RRMSE across different methods and kernel configurations for the borehole example with discretization levels $q_1 = 2$ and $q_2 \in \{2, 4, 6, 8, 10\}$. Each boxplot summarizes the results from $5q_1q_2$ independent runs with different training sets generated via maximin Latin hypercube designs. All methods were evaluated on the same set of 10,000 uniformly distributed test points.

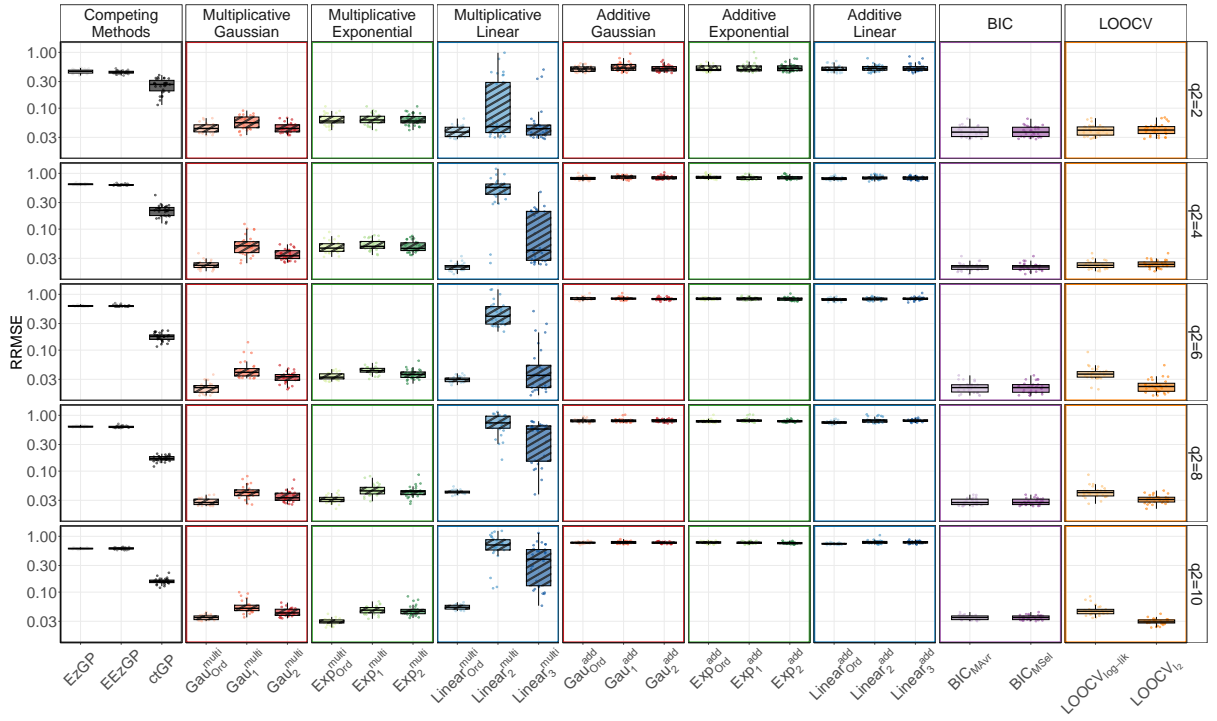


Figure S4: Comparison of RRMSE across different methods and kernel configurations for the borehole example with discretization levels $q_1 = 4$ and $q_2 \in \{2, 4, 6, 8, 10\}$, using the same experimental setup as in Figure S3.

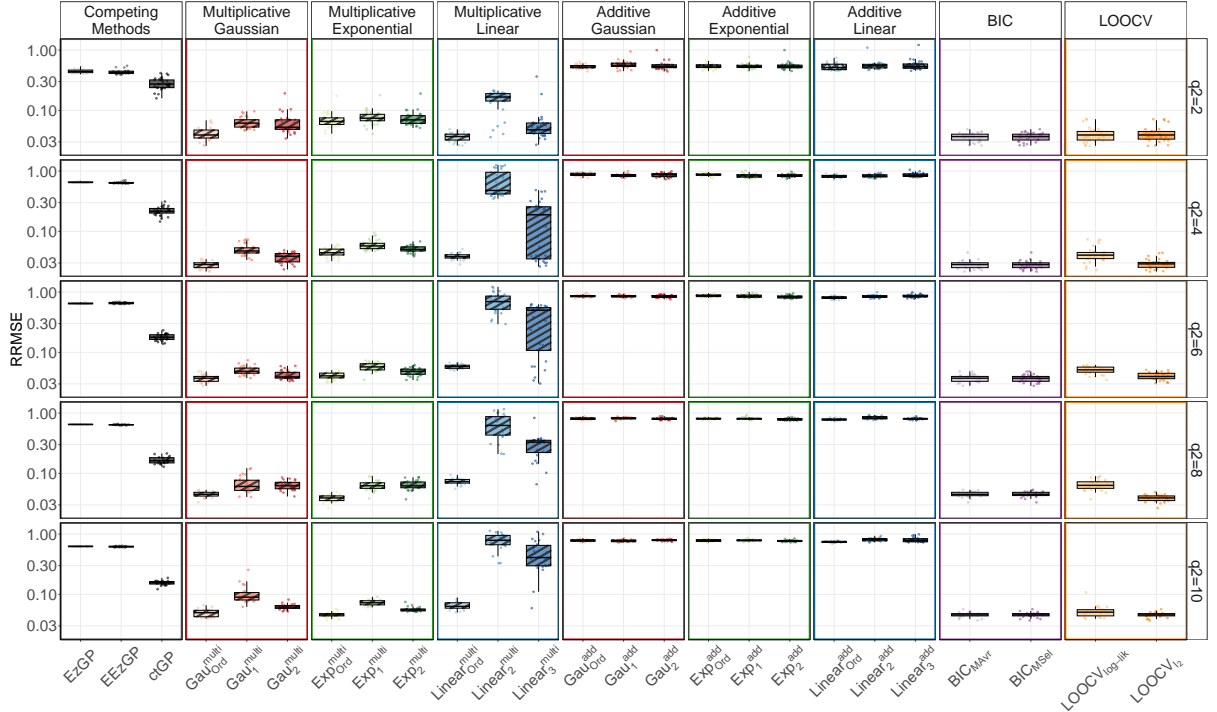
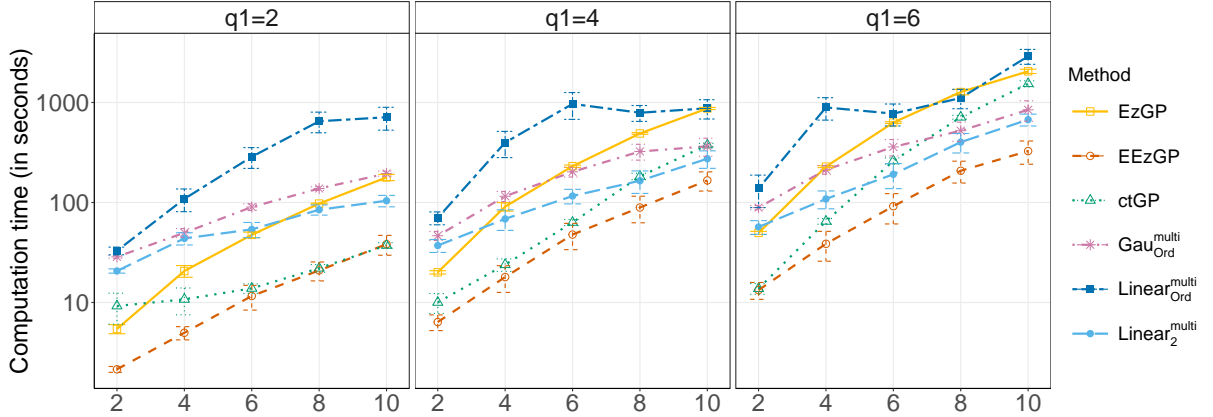
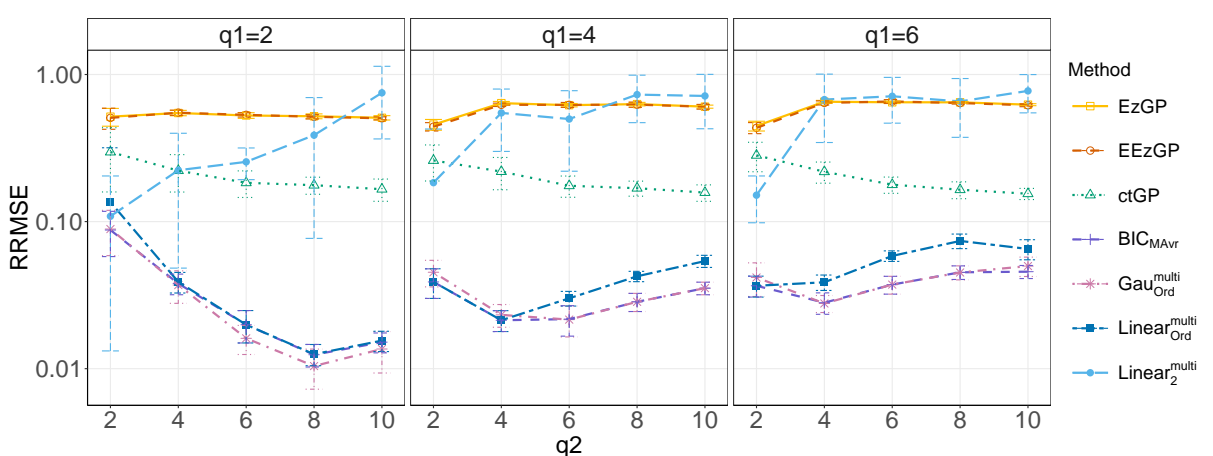


Figure S5: Comparison of RRMSE across different methods and kernel configurations for the borehole example with discretization levels $q_1 = 6$ and $q_2 \in \{2, 4, 6, 8, 10\}$, using the same experimental setup as in Figure S3.



(a) Computational time for selected methods (EzGP, EEzGP, ctGP, Gau_{Ord}^{multi}, Linear_{Ord}^{multi} and Linear₂^{multi}).



(b) RRMSE for selected methods, and additionally including the BIC-based model averaging method (BIC_{MAavr}).

Figure S6: Comparison of computational time (in seconds) and prediction accuracy for the borehole example across varying discretization levels, using the same experimental setup as in Figure S3.

Table S2: Computational time (in seconds) for three competing methods and our 18 base methods applied to the borehole problem under different discretization levels, using the same experimental setup as in Figure S3.

q_2	Time	Method																										
		EzGP			EEzGP			ctGP			Gau ^{multi}			Exp ^{multi}			Linear ^{multi}			Gau ^{add}			Exp ^{add}			Linear ^{add}		
		1-d	2-d	ord	1-d	2-d	ord	1-d	2-d	ord	1-d	2-d	ord	1-d	2-d	ord	1-d	2-d	ord	1-d	2-d	ord	1-d	2-d	ord			
$q_1 = 2$																												
2	Mean	5	2	9	29	29	29	29	29	29	21	21	33	29	29	29	29	29	29	22	22	35						
	SD	1	<1	3	1	1	1	1	1	1	1	1	3	2	2	2	2	2	2	2	2	2	6					
4	Mean	21	5	11	38	61	50	40	68	41	44	53	109	54	71	52	55	73	51	45	53	82						
	SD	3	1	3	4	7	5	4	11	4	6	8	28	9	8	7	9	10	7	6	6	25						
6	Mean	47	12	14	75	110	90	61	131	65	54	83	287	67	97	74	72	100	77	60	79	92						
	SD	3	3	2	12	5	7	8	11	8	9	8	67	14	16	11	10	24	10	11	9	13						
8	Mean	98	21	22	110	162	138	114	201	115	85	125	650	105	156	104	114	172	122	78	125	131						
	SD	1	4	2	13	9	6	11	12	11	10	8	152	14	11	16	17	26	10	15	15	24						
10	Mean	178	38	37	162	245	195	163	302	185	104	190	712	144	228	148	152	269	153	107	185	177						
	SD	13	9	2	21	10	11	14	18	10	14	12	183	29	22	27	40	31	30	22	13	35						
$q_1 = 4$																												
2	Mean	20	6	10	37	51	47	40	63	40	37	42	70	45	62	46	46	63	46	38	43	67						
	SD	1	1	2	4	6	5	3	5	3	5	6	10	6	6	6	6	7	7	6	7	15						
4	Mean	91	18	24	75	143	116	93	168	79	69	110	398	87	130	89	100	137	100	73	102	120						
	SD	9	5	3	13	17	13	14	18	12	16	16	116	18	25	11	11	22	13	13	13	29						
6	Mean	231	48	63	159	264	203	169	312	209	116	193	968	152	244	141	171	275	176	109	186	186						
	SD	6	14	4	25	22	23	15	26	28	19	20	290	31	19	29	31	38	23	26	32	49						
8	Mean	490	89	182	302	467	324	257	481	285	165	314	790	202	408	207	247	461	274	161	311	352						
	SD	10	26	13	51	70	58	51	100	37	42	42	143	56	28	50	62	47	56	39	28	85						
10	Mean	872	166	376	426	688	365	412	720	358	274	478	875	401	657	414	465	756	451	345	521	392						
	SD	22	36	15	102	107	75	65	99	62	55	95	191	69	69	35	85	71	30	60	72	102						
$q_1 = 6$																												
2	Mean	50	13	14	63	109	89	75	125	76	57	78	138	74	98	76	75	112	84	63	80	104						
	SD	2	3	2	10	4	4	9	8	9	9	10	49	14	17	11	9	22	9	10	15	23						
4	Mean	228	39	65	164	272	213	185	308	183	109	190	892	151	247	139	168	264	167	110	175	200						
	SD	5	13	4	29	22	21	11	25	18	22	19	226	35	14	33	37	33	30	28	28	66						
6	Mean	630	92	261	324	582	359	309	594	333	191	388	774	248	482	258	311	585	278	216	383	407						
	SD	12	31	19	72	77	67	38	88	55	54	70	192	63	19	71	71	69	70	52	33	77						
8	Mean	1273	208	713	550	975	522	494	1115	472	402	660	1110	533	879	541	605	1035	613	464	698	589						
	SD	80	51	32	170	204	114	103	257	80	89	149	244	106	85	40	93	144	43	65	124	163						
10	Mean	2051	327	1542	998	1485	845	993	1797	848	674	1145	2902	753	1293	756	836	1534	873	567	999	867						
	SD	101	86	107	213	295	195	185	301	149	91	214	493	152	96	148	99	104	66	119	160	172						

which implies that $\mathbf{w}_v^\top \mathbf{w}_{v'} = \mathbf{z}_v^\top \mathbf{z}_{v'}$ for any $v, v' \in \{1, \dots, a_1\}$.

For the reverse direction, we perform the QR decomposition as follows

$$\mathbf{Z}^{(1)} = \mathbf{Q}_Z \mathbf{R}_Z \quad \text{and} \quad \mathbf{W}^{(1)} = \mathbf{Q}_W \mathbf{R}_W$$

where $\mathbf{Q}_Z, \mathbf{Q}_W \in \mathbb{R}^{l_1 \times l_1}$ are orthogonal matrices, \mathbf{R}_Z and \mathbf{R}_W are upper triangular matrices with positive diagonal elements. Since $\{\mathbf{W}_v\}$ and $\{\mathbf{Z}_v\}$ are equivalent under the linear kernel, we have:

$$\mathbf{R}_W^\top \mathbf{R}_W = (\mathbf{W}^{(1)})^\top \mathbf{W}^{(1)} = (\mathbf{Z}^{(1)})^\top \mathbf{Z}^{(1)} = \mathbf{R}_Z^\top \mathbf{R}_Z.$$

According to the Cholesky decomposition and its uniqueness, we deduce that $\mathbf{R}_W = \mathbf{R}_Z$. The orthogonal matrix can be defined as $\mathbf{Q} = \mathbf{Q}_Z \mathbf{Q}_W^\top$. \square

For an isotropic kernel, the kernel value is uniquely determined by the distance between two

latent vectors. Consequently, any isometric transformation of \mathbb{R}^{l_1} results in an equivalent latent parameterization, which is formalized in Lemma S2.

Lemma S2 (Equivalence under Isotropic Kernel). *Two latent parameterizations $\{\mathbf{Wv}\}$ and $\{\mathbf{Zv}\}$ are equivalent under an isotropic kernel if and only if*

$$(\mathbf{z}_1^{(1)}, \mathbf{z}_2^{(1)}, \dots, \mathbf{z}_{a_1}^{(1)}) = \mathbf{Q}(\mathbf{w}_1^{(1)} - \mathbf{w}, \mathbf{w}_2^{(1)} - \mathbf{w}, \dots, \mathbf{w}_{a_1}^{(1)} - \mathbf{w}),$$

for some vector $\mathbf{w} \in \mathbb{R}^{l_1}$ and some orthogonal matrix $\mathbf{Q} \in \mathbb{R}^{l_1 \times l_1}$ such that $\mathbf{Q}^\top \mathbf{Q} = \mathbf{I}_{l_1 \times l_1}$.

Proof of Lemma S2. Let $\mathbf{Z}^{(1)} = (\mathbf{z}_1^{(1)}, \mathbf{z}_2^{(1)}, \dots, \mathbf{z}_{a_1}^{(1)})$ and $\mathbf{W}^{(1)} = (\mathbf{w}_1^{(1)}, \mathbf{w}_2^{(1)}, \dots, \mathbf{w}_{a_1}^{(1)})$. Suppose there exists an orthogonal matrix $\mathbf{Q} \in \mathbb{R}^{l_1 \times l_1}$ such that

$$(\mathbf{z}_1^{(1)}, \mathbf{z}_2^{(1)}, \dots, \mathbf{z}_{a_1}^{(1)}) = \mathbf{Q}(\mathbf{w}_1^{(1)} - \mathbf{w}, \mathbf{w}_2^{(1)} - \mathbf{w}, \dots, \mathbf{w}_{a_1}^{(1)} - \mathbf{w}), \quad (\text{S3})$$

where $\mathbf{w} \in \mathbb{R}^{l_1}$. In this case, parameter equivalence is guaranteed by

$$K_{\mathbf{Z}}(\mathbf{Zv}, \mathbf{Zv}') = \mathcal{K}_1\left(\left\|\mathbf{z}_{v_1}^{(1)} - \mathbf{z}_{v_1'}^{(1)}\right\|_2\right) = \mathcal{K}_1\left(\left\|\mathbf{Q}(\mathbf{w}_{v_1}^{(1)} - \mathbf{w}_{v_1'}^{(1)})\right\|_2\right) = K_{\mathbf{W}}(\mathbf{Wv}, \mathbf{Wv}'),$$

where $\mathcal{K}_1(\cdot)$ is the decreasing kernel generating function.

On the other hand, assume the above formula holds for any $v_1, v_1' \in \{1, \dots, a_1\}$. Then, we have

$$\left\|\mathbf{z}_{v_1}^{(1)} - \mathbf{z}_{v_1'}^{(1)}\right\|_2^2 = \left\|\mathbf{w}_{v_1}^{(1)} - \mathbf{w}_{v_1'}^{(1)}\right\|_2^2,$$

since $\mathcal{K}_1(\cdot)$ is a decreasing function. Note that Euclidean distance can be expressed using the inner product. By Lemma S1, we know there exists an orthogonal matrix $\mathbf{Q} \in \mathbb{R}^{l_1 \times l_1}$ such that

$$\mathbf{z}_{v_1}^{(1)} - \mathbf{z}_{v_1'}^{(1)} = \mathbf{Q}(\mathbf{w}_{v_1}^{(1)} - \mathbf{w}_{v_1'}^{(1)}),$$

for any $v_1, v_1' \in \{1, \dots, a_1\}$. Thus, defining $\mathbf{w} = \mathbf{Q}^\top \mathbf{z}_{v_1}^{(1)} - \mathbf{w}_{v_1}^{(1)}$ results in a constant vector \mathbf{w} , independent of v_1 , based on the formula above. Finally, the defined \mathbf{Q} and \mathbf{w} ensure that (S3) holds, which justifies the reverse direction as well. This completes the proof. \square

References

Ben-Ari, E. N. and Steinberg, D. M. (2007), “Modeling data from computer experiments: An empirical comparison of kriging with MARS and projection pursuit regression,” *Quality Engineering*, 19, 327–338.

Harper, W. V. and Gupta, S. K. (1983), “Sensitivity/uncertainty analysis of a borehole scenario comparing Latin hypercube sampling and deterministic sensitivity approaches,” Tech. rep., Battelle Memorial Inst., Columbus, OH (USA). Office of Nuclear Waste Isolation.

Joseph, V. R., Gul, E., and Ba, S. (2015), “Maximum projection designs for computer experiments,” *Biometrika*, 102, 371–380.

— (2020), “Designing computer experiments with multiple types of factors: The MaxPro approach,” *Journal of Quality Technology*, 52, 343–354.

Morris, M. D., Mitchell, T. J., and Ylvisaker, D. (1993), “Bayesian design and analysis of computer experiments: Use of derivatives in surface prediction,” *Technometrics*, 35, 243–255.

Santner, T. J., Williams, B. J., Notz, W. I., and Williams, B. J. (2003), *The Design and Analysis of Computer Experiments*, vol. 1, Springer.

Zhang, Y., Tao, S., Chen, W., and Apley, D. W. (2020), “A latent variable approach to Gaussian process modeling with qualitative and quantitative factors,” *Technometrics*, 62, 291–302.